JCI The Journal of Clinical Investigation

Local TNF causes NFATc1-dependent cholesterol-mediated podocyte injury

Christopher E. Pedigo, … , Sandra Merscher, Alessia Fornoni

J Clin Invest. 2016;126(9):3336-3350. https://doi.org/10.1172/JCI85939.

Research Article **Inflammation**

High levels of circulating TNF and its receptors, TNFR1 and TNFR2, predict the progression of diabetic kidney disease (DKD), but their contribution to organ damage in DKD remains largely unknown. Here, we investigated the function of local and systemic TNF in podocyte injury. We cultured human podocytes with sera collected from DKD patients, who displayed elevated TNF levels, and focal segmental glomerulosclerosis (FSGS) patients, whose TNF levels resembled those of healthy patients. Exogenous TNF administration or local TNF expression was equally sufficient to cause free cholesterol–dependent apoptosis in podocytes by acting through a dual mechanism that required a reduction in ATP-binding cassette transporter A1–mediated (ABCA1-mediated) cholesterol efflux and reduced cholesterol esterification by sterol-*O*-acyltransferase 1 (SOAT1). TNF-induced albuminuria was aggravated in mice with podocyte-specific ABCA1 deficiency and was partially prevented by cholesterol depletion with cyclodextrin. TNF-stimulated free cholesterol–dependent apoptosis in podocytes was mediated by nuclear factor of activated T cells 1 (NFATc1). ABCA1 overexpression or cholesterol depletion was sufficient to reduce albuminuria in mice with podocyte-specific NFATc1 activation. Our data implicate an NFATc1/ABCA1-dependent mechanism in which local TNF is sufficient to cause free cholesterol–dependent podocyte injury irrespective of TNF, TNFR1, or TNFR2 serum levels.

Find the latest version:

https://jci.me/85939/pdf

Local TNF causes NFATc1-dependent cholesterol-mediated podocyte injury

Christopher E. Pedigo,[1,2] Gloria Michelle Ducasa,[1,2] Farah Leclercq,[1,2] Alexis Sloan,[1,2] Alla Mitrofanova,[1,2] Tahreem Hashmi,[1,2] Judith Molina-David,[1,2] Mengyuan Ge,[1,2] Mariann I. Lassenius,[3,4,5] Carol Forsblom,[3,4,5] Markku Lehto,[3,4,5] Per-Henrik Groop,[3,4,5,6] Matthias Kretzler,[7] Sean Eddy,[7] Sebastian Martini,[7] Heather Reich,[8] Patricia Wahl,[1,2] GianMarco Ghiggeri,[9] Christian Faul,[1,2] George W. Burke III,[2,10,11] Oliver Kretz,[12,13] Tobias B. Huber,[12,14,15] Armando J. Mendez,[11] Sandra Merscher,[1,2] and Alessia Fornoni[1,2]

[1]Division of Nephrology and Hypertension and [2]Peggy and Harold Katz Drug Discovery Center, University of Miami Miller School of Medicine, Miami, Florida, USA. [3]Folkhälsan Institute of Genetics, Folkhälsan Research Center, Helsinki, Finland. [4]Abdominal Center Nephrology and [5]Research Programs Unit–Diabetes and Obesity, University of Helsinki and Helsinki University Central Hospital, Helsinki, Finland. [6]Baker IDI Heart and Diabetes Institute, Melbourne, Australia. [7]Department of Internal Medicine, Division of Nephrology, University of Michigan, Ann Arbor, Michigan, USA. [8]Division of Nephrology, University of Toronto, Toronto, Ontario, Canada. [9]Division of Nephrology, Giannina Gaslini Children's Hospital, Genoa, Italy. [10]Department of Surgery and [11]Diabetes Research Institute University of Miami Miller School of Medicine, Miami, Florida, USA. [12]Renal Division, Medical Center–University of Freiburg, Faculty of Medicine, Freiburg, Germany. [13]Department of Neuroanatomy, Faculty of Medicine, University of Freiburg, Germany. [14]BIOSS Centre for Biological Signalling Studies, Albert-Ludwigs University, Freiburg, Germany. [15]Freiburg Institute for Advanced Studies and Center for Biological Systems Analysis (ZBSA), Freiburg, Germany.

High levels of circulating TNF and its receptors, TNFR1 and TNFR2, predict the progression of diabetic kidney disease (DKD), but their contribution to organ damage in DKD remains largely unknown. Here, we investigated the function of local and systemic TNF in podocyte injury. We cultured human podocytes with sera collected from DKD patients, who displayed elevated TNF levels, and focal segmental glomerulosclerosis (FSGS) patients, whose TNF levels resembled those of healthy patients. Exogenous TNF administration or local TNF expression was equally sufficient to cause free cholesterol–dependent apoptosis in podocytes by acting through a dual mechanism that required a reduction in ATP-binding cassette transporter A1–mediated (ABCA1-mediated) cholesterol efflux and reduced cholesterol esterification by sterol-*O*-acyltransferase 1 (SOAT1). TNF-induced albuminuria was aggravated in mice with podocyte-specific ABCA1 deficiency and was partially prevented by cholesterol depletion with cyclodextrin. TNF-stimulated free cholesterol–dependent apoptosis in podocytes was mediated by nuclear factor of activated T cells 1 (NFATc1). ABCA1 overexpression or cholesterol depletion was sufficient to reduce albuminuria in mice with podocyte-specific NFATc1 activation. Our data implicate an NFATc1/ABCA1-dependent mechanism in which local TNF is sufficient to cause free cholesterol–dependent podocyte injury irrespective of TNF, TNFR1, or TNFR2 serum levels.

Introduction

Chronic low-grade inflammation and elevated TNF levels have been associated with several diseases, such as rheumatoid arthritis (1), multiple sclerosis (2), and atherosclerosis (3). However, the complex nature of systemic and local TNF has made it difficult to dissect how TNF contributes to disease development and/or progression. This has been further compounded by the fact that commonly used TNF inhibitors may bind to both systemic and local TNF (4). It has been proposed that systemic/serum TNF may be spillover from locally produced TNF within an affected tissue (5). Circulating TNF, TNF receptor 1 (TNFR1), and TNF receptor 2 (TNFR2) are associated with the development (6–8) and the progression of diabetic kidney disease (DKD) (9–12). However, a causal role for these biomarkers has not been established. Clinical studies have suggested that TNF inhibition may be efficacious in a subset of patients (13, 14) affected by focal segmental glomerulosclerosis (FSGS), a rare kidney disease in which the role of circulating TNF, TNFR1, and TNFR2 in predicting clinical outcome has yet to be established. Nevertheless, these clinical studies were plagued by variable outcomes, suggesting the importance of appropriate patient stratification when studying targeted therapies in highly heterogeneous diseases. Furthermore, as concerns about the high risk for infection and malignancies associated with anti-TNF therapy remain high, the identification of downstream mechanisms and other drug targets will provide new opportunities for the development of safer therapeutic strategies.

Altered cholesterol efflux has been reported to contribute to several diseases, including atherosclerosis (15), nonalcoholic fatty liver disease, and Tangier disease (16). We recently reported that glomeruli isolated from patients with type 2 diabetes and DKD are characterized by reduced expression of ATP-binding cassette transporter A1 (ABCA1) (17), a transmembrane protein involved in cholesterol efflux. These observations suggest that

Conflict of interest: G.W. Burke III, A. Fornoni, and S. Merscher are inventors on pending or issued patents aimed to diagnose or treat proteinuric renal diseases. They stand to gain royalties from their future commercialization. A. Fornoni is consultant for Hoffman-La Roche, Genentech, Janssen, Mesoblast, Abbvie, Boehringer Ingelheim, Alexion, Bristol-Myers Squibb, Pfizer, Astellas, Variant Pharmaceutical, and Mallinckrodt. C. Faul has served as a consultant for Ultragenyx and has received research support from U3 Pharma GmbH.

Submitted: December 14, 2015; **Accepted:** May 26, 2016.

Reference information: *J Clin Invest*. 2016;126(9):3336–3350. doi:10.1172/JCI85939.

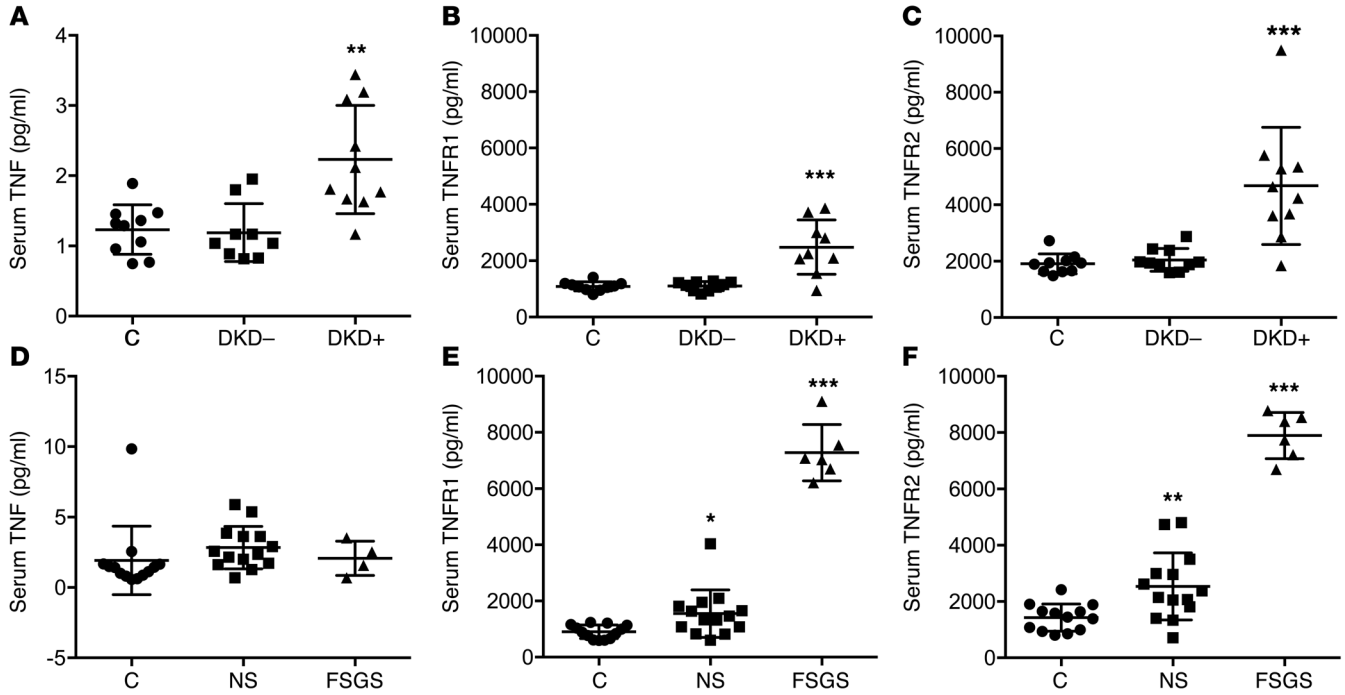

Figure 1. Serum TNF, TNFR1, and TNFR2 levels in patients with nephrotic syndrome, FSGS, and DKD. (**A**–**C**) ELISA-based quantification of serum TNF (**A**), TNFR1 (**B**), and TNFR2 (**C**) levels in 10 patients with diabetic kidney disease (DKD+), 10 patients with diabetes (DKD–), and 10 healthy patients (C). One-way ANOVA; $^{**}P < 0.01$ DKD+ vs. C; $^{***}P < 0.001$ DKD+ vs. C. (**D**–**F**) ELISA-based quantification of serum TNF (**D**), TNFR1 (**E**), and TNFR2 (**F**) levels in patients with biopsy-proven FSGS (FSGS, $n = 6$), patients with nephrotic syndrome (NS, $n = 14$), and healthy patients (C, $n = 14$). One-way ANOVA; $^{*}P < 0.05$ NS vs. C; $^{**}P < 0.01$ FSGS vs. C; $^{***}P < 0.001$ FSGS vs. C.

local cholesterol accumulation due to decreased cholesterol efflux may contribute to the pathogenesis of DKD. Concurrent with this observation, lipid deposition specifically in podocytes has been observed in kidney biopsies from patients with DKD, and altered glomerular expression of genes involved in lipid metabolism such as *ABCA1* correlated with inflammatory markers and estimated glomerular filtration rate (eGFR) (18). Several immunosuppressive regimens are commonly used to treat proteinuric glomerular disorders, such as cyclosporin A (CsA) (19), a pharmacological inhibitor of calcineurin that is an upstream regulator of nuclear factor of activated T cells (NFAT) signaling (20, 21). Interestingly, CsA may be a direct modulator of podocyte function irrespectively of its systemic immunological effects (22). Since the *ABCA1* promoter region contains an NFAT response element (23), it is possible that NFAT activation is mechanistically linked to ABCA1 expression and cholesterol accumulation in kidney disease.

Based on these clinical and experimental observations, we hypothesized that TNF causes cholesterol-mediated podocyte injury in FSGS and DKD in an NFAT-dependent manner. We show that podocyte apoptosis caused by the exposure of human podocytes to sera from patients with DKD or FSGS is associated with increased podocyte TNF production that is independent of circulating TNF. We further demonstrate with in vitro and in vivo studies that podocyte expression of TNF causes NFAT-mediated ABCA1 repression and reduced sterol-*O*-acyltransferase 1 (SOAT1) activity leading to free cholesterol–mediated podocyte apoptosis. Thus, our data identify a novel pathway linking key clinical and experimental findings that support targeting of TNF, NFAT, ABCA1, SOAT1, or free cholesterol in patients with FSGS or DKD, irrespectively of circulating levels of TNF, TNFR1, or TNFR2.

Results

Increased serum TNFR1 and TNFR2 levels are detected in DKD and FSGS, whereas increased TNF levels are detected only in DKD. Circulating levels of TNF, TNFR1, and TNFR2 predict chronic kidney disease (CKD) progression in patients with type 1 diabetes (T1D) (9, 11) and type 2 diabetes (10, 12). We studied a small cohort of patients with T1D and kidney disease (DKD+) enrolled in the FinnDiane Study ($n = 10$ per group) (17) and demonstrated that these patients had elevated TNF, TNFR1, and TNFR2 serum levels when compared with patients with T1D without kidney disease (DKD–) who were matched for age, fasting glycemia, duration of diabetes, total cholesterol, HDL cholesterol, LDL cholesterol, and triglycerides and compared with age- and sex-matched healthy controls (Figure 1, A–C). To determine whether this phenomenon was specific to DKD, we determined serum levels of TNF, TNFR1, and TNFR2 from healthy patient controls ($n = 14$), patients with steroid-dependent nephrotic syndrome (NS) ($n = 14$), and patients with biopsy-proven primary FSGS ($n = 6$). We found that serum TNF levels were unaltered in patients with NS and FSGS (Figure 1D). Unaltered TNF levels were confirmed in a larger and well-characterized cohort of patients affected by FSGS enrolled in the Nephrotic Syndrome Study Network (NEPTUNE) study (Supplemental Figure 1; supplemental material available online with this article; doi:10.1172/JCI85939DS1). However, serum TNFR1 and TNFR2 were modestly increased in patients with NS and further augmented in patients with FSGS (Figure 1, E and F).

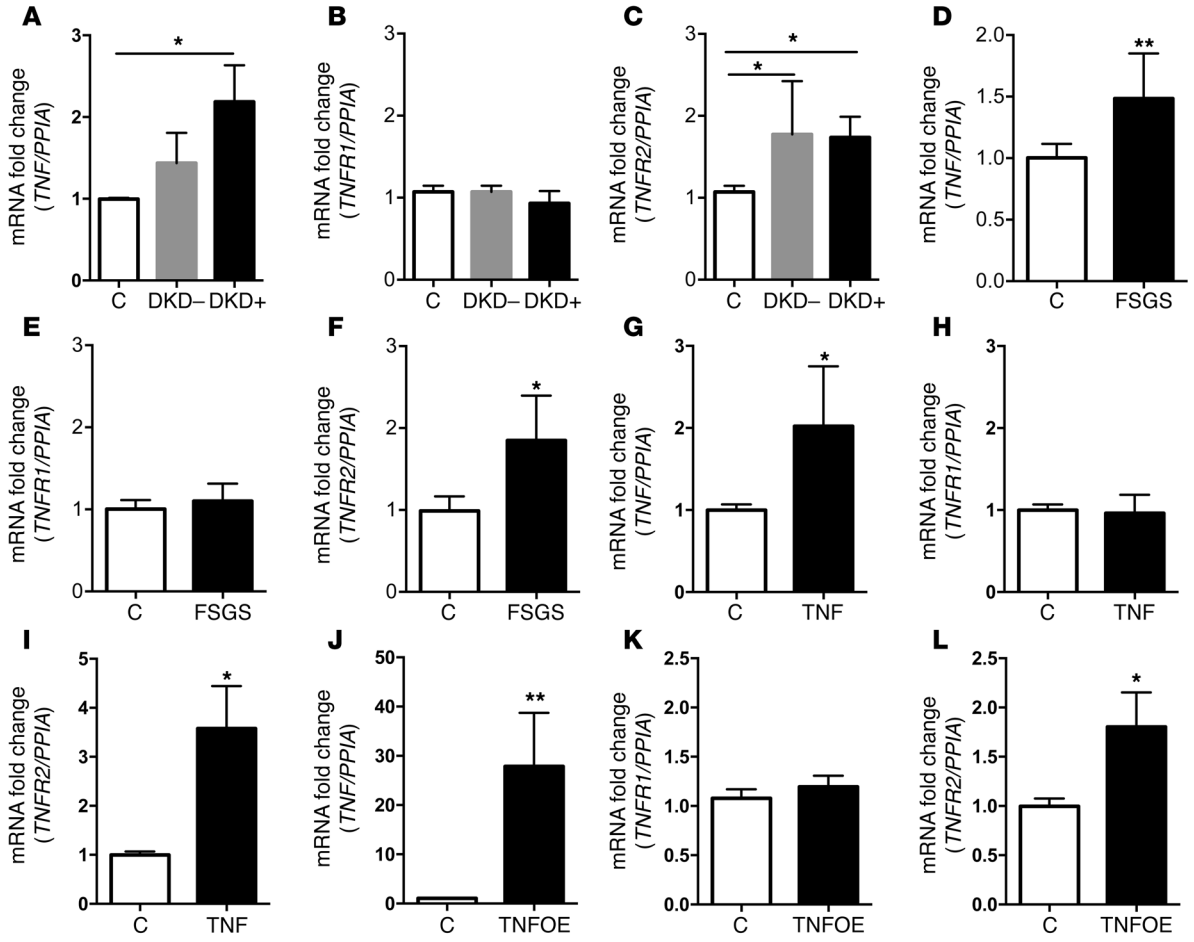

Figure 2. Analysis of podocyte TNF, TNFR1, and TNFR2 expression after treatment with serum from patients with FSGS or DKD, after exposure to TNF or after TNF overexpression. (**A**–**C**) Quantitative real-time (RT) PCR analysis of *TNF* (**A**), *TNFR1* (**B**), and *TNFR2* (**C**) expression in podocytes exposed to pooled sera from patients with diabetic kidney disease (DKD+) or diabetes (DKD–) and healthy controls (C) ($n = 3$). One-way ANOVA; $^*P < 0.05$ DKD–, DKD+ vs. C. (**D**–**F**) Quantitative RT-PCR analysis of *TNF* (**D**), *TNFR1* (**E**), and *TNFR2* (**F**) expression in podocytes exposed to sera from individual patients with FSGS ($n = 6$) and serum from healthy controls (C, $n = 6$). Two-tailed Student's *t* test; $^*P < 0.05$. $^{**}P < 0.01$. (**G**–**I**) Quantitative RT-PCR analysis of *TNF* (**G**), *TNFR1* (**H**), and *TNFR2* (**I**) expression in podocytes exposed to recombinant human TNF ($n = 3$). Two-tailed Student's *t* test; $^*P < 0.05$. (**J**–**L**) Quantitative RT-PCR analysis of *TNF* (**J**), *TNFR1* (**K**), and *TNFR2* (**L**) expression in podocytes overexpressing TNF (TNFOE) compared with empty vector controls (C) ($n = 3$). Two-tailed Student's *t* test; $^*P < 0.05$, $^{**}P < 0.01$.

Podocyte expression of TNF and TNFR2 is induced by DKD and FSGS sera as well as by soluble or podocyte-derived TNF. We previously described that human podocytes exposed to DKD+ sera are characterized by a distinct microarray signature compared with podocytes exposed to DKD– and healthy control sera. One of the clusters of genes significantly regulated in podocytes after exposure to DKD+ sera contained genes involved in cytokine–cytokine receptor interaction (17). This observation led us to investigate whether exposure to DKD+ sera may cause changes in the podocyte expression (local expression) of TNF and/or its receptors. Using quantitative real-time PCR analysis, we showed that podocytes exposed to DKD+ sera had significantly increased mRNA expression levels of *TNF* and *TNFR2* compared with controls (Figure 2, A and C), while *TNFR1* mRNA expression levels remained unchanged (Figure 2B). Increased TNF expression levels were confirmed by Western blot analysis of DKD+ sera–treated podocytes (Supplemental Figure 2). TNFR2 was increased when podocytes were exposed to sera from patients with diabetes irrespectively of the presence or absence of DKD (Figure 2C). This mRNA profile was recapitulated in FSGS patient sera–treated podocytes, demonstrating increased *TNF* and *TNFR2* (Figure 2, D and F) with no changes in *TNFR1* expression (Figure 2E). These results indicate that increases in the expression of *TNF* and *TNFR2* in sera-treated podocytes occur upon exposure to both DKD+ and FSGS sera irrespectively of serum TNF levels. We then aimed to determine whether treatment of human podocytes with exogenous TNF would also increase local TNF expression. Similar to what was observed in DKD+ patient sera–treated podocytes, TNF-treated podocytes showed increased local TNF (Figure 2G and Supplemental Figure 3) and *TNFR2* expression levels (Figure 2I) without affecting *TNFR1* (Figure 2H). To determine the role of local TNF expression in the expression of *TNFR1* and *TNFR2*, lentiviral infection to overexpress TNF (TNFOE) was used (Supplemental Figure 4). Interestingly, increased local TNF expression led to increased expression of *TNFR2* (Figure 2L) but not *TNFR1* (Figure 2K), similarly to what we observed

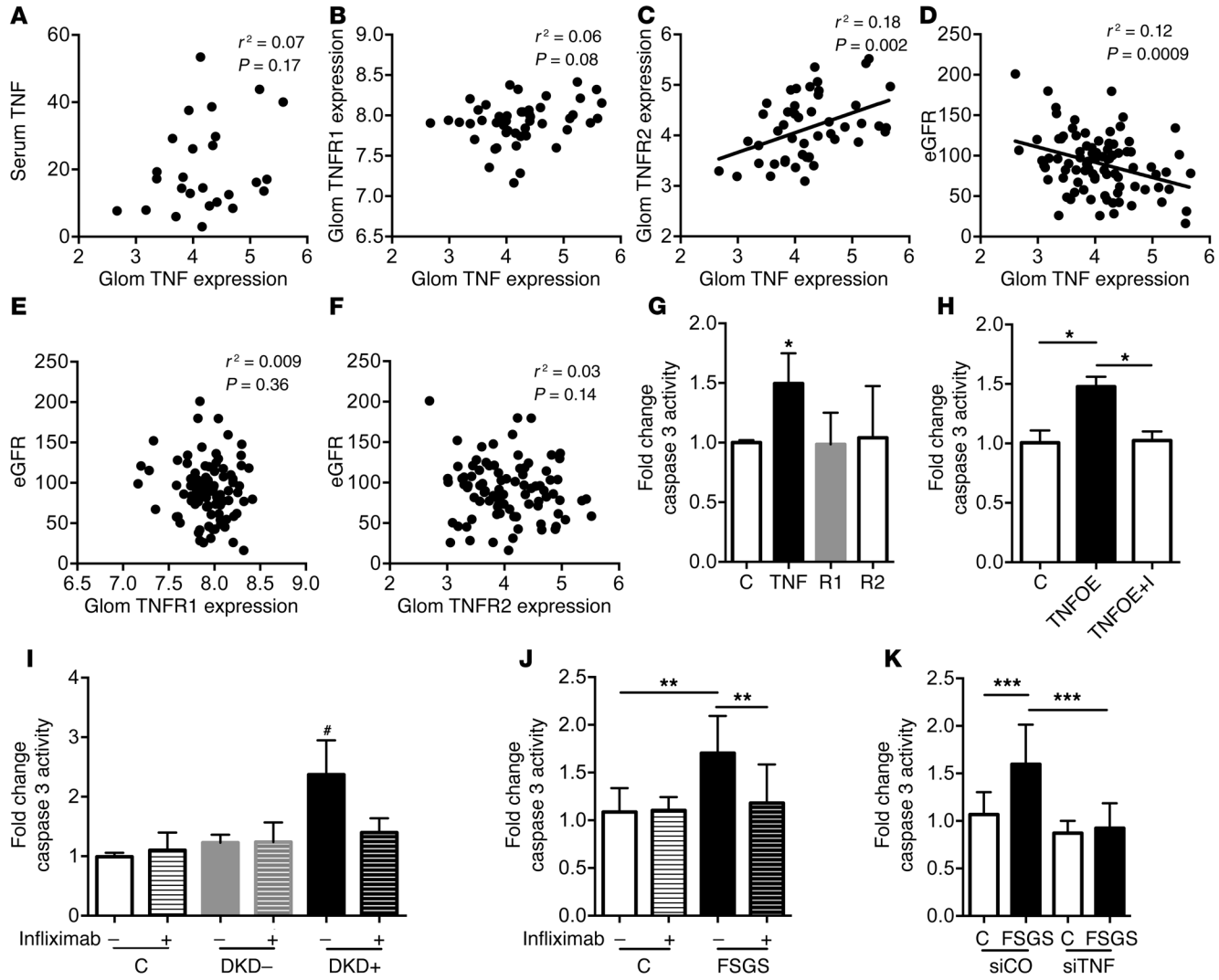

Figure 3. Glomerular TNF expression correlates to eGFR and is sufficient to cause podocyte apoptosis. (**A**) Serum TNF levels from patients with FSGS from the NEPTUNE cohort do not correlate with glomerular TNF expression in kidney biopsies as determined by microarray analysis. (**B**–**F**) Microarray analysis of glomeruli from patients enrolled in the NEPTUNE cohort reveals that glomerular TNF expression does not correlate with TNFR1 expression (**B**), positively correlates with TNFR2 expression (**C**), and inversely correlates with eGFR (**D**). Neither TNFR1 expression (**E**) nor TNFR2 expression (**F**) correlates with eGFR. (**G**) Caspase 3 activity was measured in cultured human podocytes that were exposed to recombinant human TNF, TNFR1, or TNFR2. TNF but not TNFR1 or TNFR2 increased caspase 3 activity compared with untreated controls (C). One-way ANOVA; $^*P < 0.05$. (**H**) TNF overexpression (TNFOE) in human podocytes causes increased cleaved caspase 3 activity compared with empty vector controls (C), which was prevented by the TNF inhibitor infliximab (I) ($n = 4$). One-way ANOVA; $^*P < 0.05$. (**I**) Treatment of human podocytes with infliximab prevents DKD+ sera–induced cleaved caspase 3 activity ($n = 4$). One-way ANOVA; $^{\#}P < 0.01$ DKD+ without I vs. C, C with I, DKD–, DKD– with I, DKD+ with I. (**J**) Treatment of human podocytes with infliximab prevents FSGS sera–induced ($n = 6$) caspase 3 activity ($n = 3$). One-way ANOVA; $^{**}P < 0.01$. (**K**) Knockdown of TNF (siTNF) prevents cleaved caspase 3 activity in podocytes exposed to serum from patients with FSGS ($n = 7$) compared with siCO-treated podocytes ($n = 3$). One-way ANOVA; $^{***}P < 0.001$.

when podocytes were treated with DKD sera, FSGS sera, or recombinant human TNF (Figure 2, A–I).

Glomerular TNF but not TNFR1 or TNFR2 inversely correlates with eGFR. To support our in vitro findings, we obtained data of the microarray analysis of glomerular biopsies from patients enrolled in the NEPTUNE study. Serum TNF levels did not correlate with glomerular *TNF* expression (Figure 3A). Consistent with our findings in DKD and FSGS patient sera–treated podocytes, glomerular *TNF* expression in the NEPTUNE cohort did not correlate with *TNFR1* expression (Figure 3B) but positively correlated with glomerular *TNFR2* expression (Figure 3C). To determine whether this *TNF* expression profile was associated with clinical parameters, we performed correlation analysis between eGFR of patients at enrollment and *TNF, TNFR1,* and *TNFR2* in the FSGS and minimal-change disease NEPTUNE cohort. *TNFR1* and *TNFR2* expression did not correlate with eGFR (Figure 3, E and F). However, local *TNF* expression significantly correlated with reduced eGFR (Figure 3D). These data indicate a possible role for glomerular *TNF* but not *TNFR1* or *TNFR2* in the progression of CKD in a subset of patients with FSGS.

Local TNF causes DKD and FSGS sera–induced podocyte apoptosis. Consistent with the clinical data supporting a role of TNF in podocyte injury, in vitro experiments demonstrated that TNF but not TNFR1 or TNFR2 causes increased cleaved caspase 3 activi-

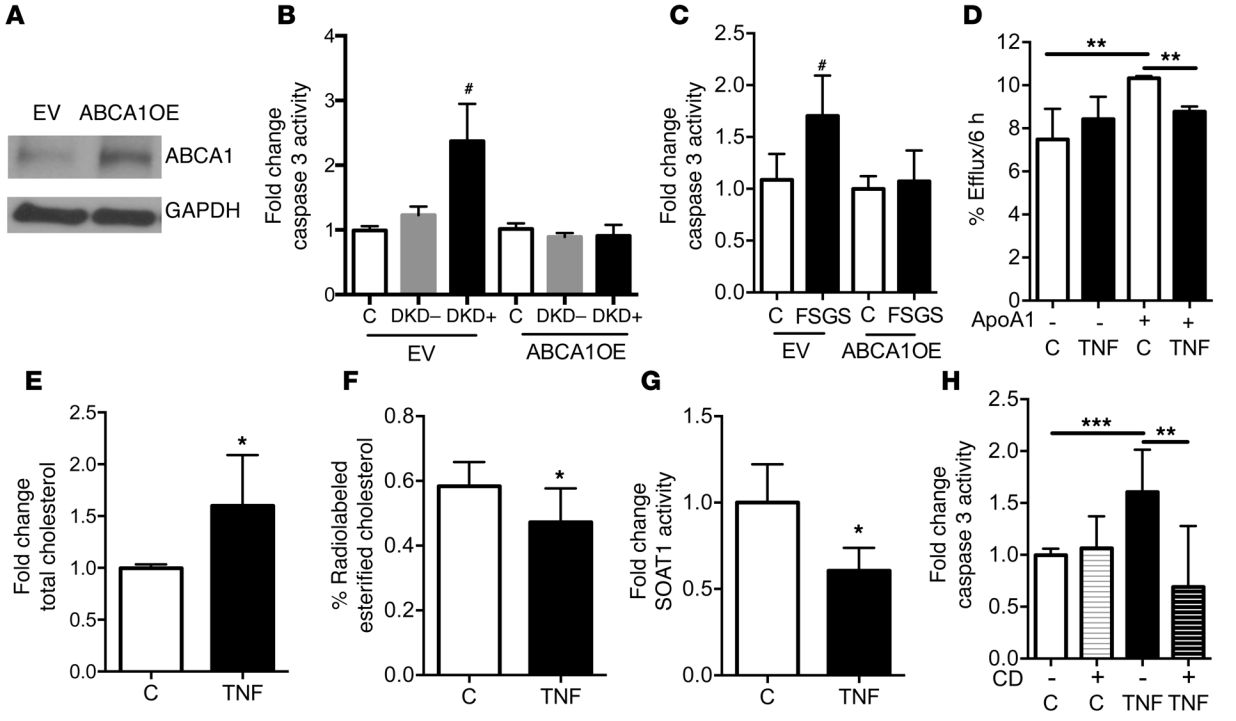

Figure 4. *ABCA1* overexpression is sufficient to protect from sera-induced podocyte injury, and TNF treatment alters human podocyte cholesterol homeostasis. (**A**) Representative Western blot analysis showing that ABCA1-overexpressing (ABCA1OE) podocytes have increased ABCA1 protein compared with empty vector (EV) controls. GAPDH is the loading control. (**B**) Cleaved caspase 3 analysis in DKD patient sera–treated EV and ABCA1OE. One-way ANOVA; $^{\#}P < 0.05$ compared with all columns. (**C**) Cleaved caspase 3 analysis in FSGS patient sera–treated EV and ABCA1OE. One-way ANOVA; $^{\#}P < 0.05$ compared with all columns. (**D**) TNF treatment of cultured human podocytes results in significant reduction of ABCA1-mediated ApoA1-dependent cholesterol efflux compared with untreated controls (C) ($n = 4$). One-way ANOVA; $^{**}P < 0.01$. (**E**) TNF treatment of cultured human podocytes leads to increased total cholesterol content compared with untreated controls ($n = 3$). Two-tailed Student's t test; $^{*}P < 0.05$. (**F**) TNF treatment of cultured human podocytes leads to reduced esterified cholesterol content compared with untreated controls ($n = 4$). Two-tailed Student's t test; $^{*}P < 0.05$. (**G**) TNF treatment of cultured human podocytes leads to reduced SOAT activity compared with untreated controls ($n = 4$). Two-tailed Student's t test; $^{*}P < 0.05$. (**H**) Pretreatment with CD prevents TNF-induced caspase 3 activity in cultured human podocytes compared with TNF-treated human podocytes ($n = 5$). One-way ANOVA; $^{**}P < 0.01$, $^{***}P < 0.001$.

ty (Figure 3G). As exogenous TNF increases local TNF expression and causes podocyte apoptosis, we also studied the role of local TNF in causing podocyte injury. TNFOE was sufficient to significantly increase podocyte caspase 3 activity, and treatment with a monoclonal antibody against human TNF, infliximab, prevented TNFOE-induced caspase 3 activity (Figure 3H). Likewise, infliximab prevented increased caspase 3 activity (Figure 3, I and J) and cytotoxicity (Supplemental Figure 5, A and B) induced by treatment of human podocytes with sera from patients with DKD and FSGS. Podocytes expressing siRNA to silence TNF (siTNF) were generated (Supplemental Figure 6). Scramble siRNA control (siCO) podocytes were susceptible to, whereas siTNF podocytes were protected from, apoptosis (Figure 3K) and cytotoxicity (Supplemental Figure 5C) upon exposure to sera from patients with FSGS. Furthermore, siTNF protected from DKD+ patient sera–mediated reduced cholesterol efflux (Supplemental Figure 7). To further understand the mechanism of local TNF–induced injury, we demonstrated that TNFR1 but not TNFR2 inhibition prevents soluble TNF to cause podocyte apoptosis (Supplemental Figure 8A) whereas neither TNFR1 nor TNFR2 inhibition prevented TNFOE-induced apoptosis (Supplemental Figure 8B). These results highlight that local TNF expression is sufficient to cause podocyte injury and is likely independent of its receptors.

Increased local TNF expression in glomeruli from FSGS patients correlates with reduced ABCA1 expression. Analysis by GWAS and microarray analysis of glomeruli of patients with CKD demonstrated that the activation of key inflammatory pathways (24) is shared between clinical and experimental DKD (25). We recently demonstrated that glomerular biopsies from patients with DKD are characterized by reduced *ABCA1* expression (17). To determine whether altered *ABCA1* expression also occurs in glomeruli from patients with FSGS and is associated with local *TNF* expression, we analyzed glomerular expression data available from the European Renal cDNA Bank (ERCB) from kidney biopsies of NS patients (26), including FSGS ($n = 24$) and minimal-change disease ($n = 14$). Increased glomerular *TNF* expression correlated with reduced glomerular *ABCA1* expression (Supplemental Figure 9). To further investigate the causative role of ABCA1 in serum-mediated apoptosis, we generated *ABCA1*-overexpressing (ABCA1OE) podocytes (Figure 4A). Supporting our clinical findings, *ABCA1* overexpression prevented DKD and FSGS sera–induced podocyte apoptosis (Figure 4, B and C) and cytotoxicity (Supplemental Figure 5, D and E).

TNF treatment of human podocytes inhibits ABCA1-dependent cholesterol efflux, leading to apoptosis. Given that TNF may affect *ABCA1* expression in other organs (27, 28), that TNF induces

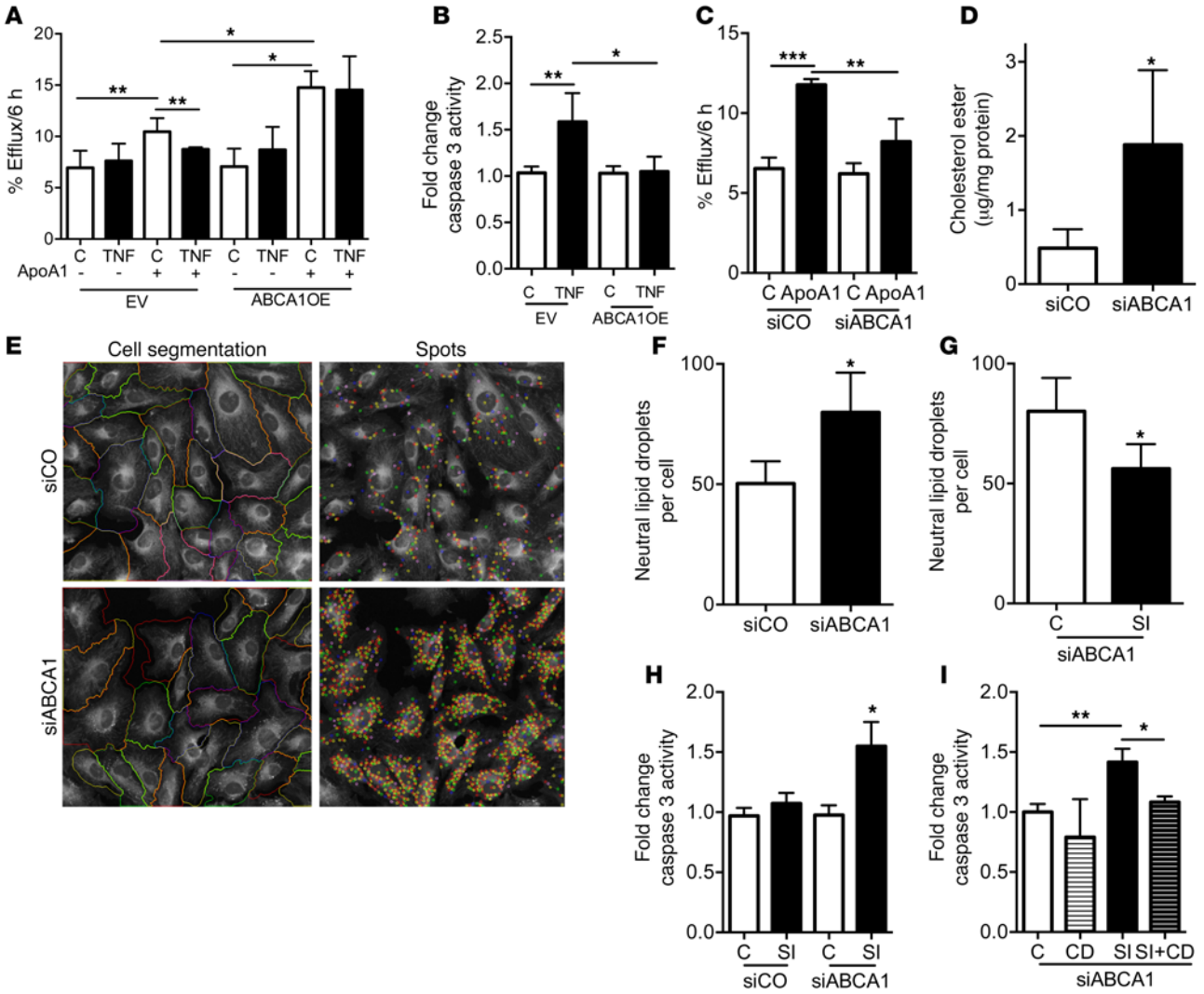

Figure 5. Reduced ABCA1-mediated cholesterol efflux and reduced SOAT1 activity cause free cholesterol–mediated podocyte apoptosis. (**A**) Cholesterol efflux is increased in empty vector podocytes (EV) in the presence of ApoA1. TNF treatment of EV results in reduced ABCA1-mediated cholesterol efflux to ApoA1. ABCA1-overexpressing podocytes (ABCA1OE) have increased cholesterol efflux to ApoA1 compared with EV, which remains unaffected by TNF treatment (n = 3). One-way ANOVA; *P < 0.05, **P < 0.01, ***P < 0.001. (**B**) TNF treatment of ABCA1OE does not result in increased caspase 3 activity compared with TNF-treated EV controls (n = 4). One-way ANOVA; *P < 0.05, **P < 0.01. (**C**) siABCA1 podocytes have reduced cholesterol efflux to ApoA1 compared with siCO (n = 3). One-way ANOVA; **P < 0.01, ***P < 0.001. (**D**) siABCA1 podocytes have increased esterified cholesterol mass compared with siCO (n = 3). Two-tailed Student's t test; *P < 0.05. (**E**) Representative confocal image (original magnification, ×20) using Opera HCS to analyze neutral lipid droplet staining (right panels) and cell segmentation (left panels) in siCO (top panels) and siABCA1 podocytes (bottom panels). (**F**) Bar graph of the quantitative lipid droplet analysis using Acapella demonstrating increased spots per cell in siABCA1 cells compared with controls (n = 5). Two-tailed Student's t test; *P < 0.05. (**G**) Bar graph of the quantitative analysis demonstrating that siABCA1 podocytes treated with SOAT1 inhibitor (SI) have a reduced number of lipid droplet spots per cell (n = 4) when compared with untreated control (C). Two-tailed Student's t test; *P < 0.05. (**H**) SI increases cleaved caspase 3 activity in siABCA1 but not siCO podocytes (n = 3). One-way ANOVA; *P < 0.05. (**I**) Pretreatment with CD prevented SI-induced caspase 3 activity in siABCA1 podocytes (n = 4). One-way ANOVA; *P < 0.05, **P < 0.01.

apoptosis in podocytes isolated from diabetic mice (29), and that ABCA1-dependent cholesterol efflux impairment in DKD is associated with podocyte apoptosis (17), we tested the hypothesis that TNF causes podocyte apoptosis by reducing ABCA1-mediated cholesterol efflux to ApoA1 leading to cholesterol accumulation. As expected, TNF treatment and TNFOE reduced *ABCA1* mRNA expression (Supplemental Figure 10). To determine the effect of TNF on ABCA1-mediated cholesterol efflux via ApoA1, podocytes were exposed to [^{3}H]-cholesterol in the presence or absence of TNF, and ApoA1-mediated cholesterol efflux was measured. TNF treatment of podocytes significantly reduced ApoA1-mediated cholesterol efflux (Figure 4D). Quantitative enzymatic analysis of cholesterol content revealed significant increases in total cholesterol content in TNF-treated cells compared with untreated controls (Figure 4E). This occurred in association with a significant reduction in the esterified cholesterol pool (Figure 4F). To further define the mechanism by which TNF reduces the esterified cholesterol pool, podocytes were exposed to [^{14}C]-oleic acid, and SOAT1 activity was measured by assessment of [^{14}C] incorporation into the esterified cholesterol pool. SOAT1 activity was signifi-

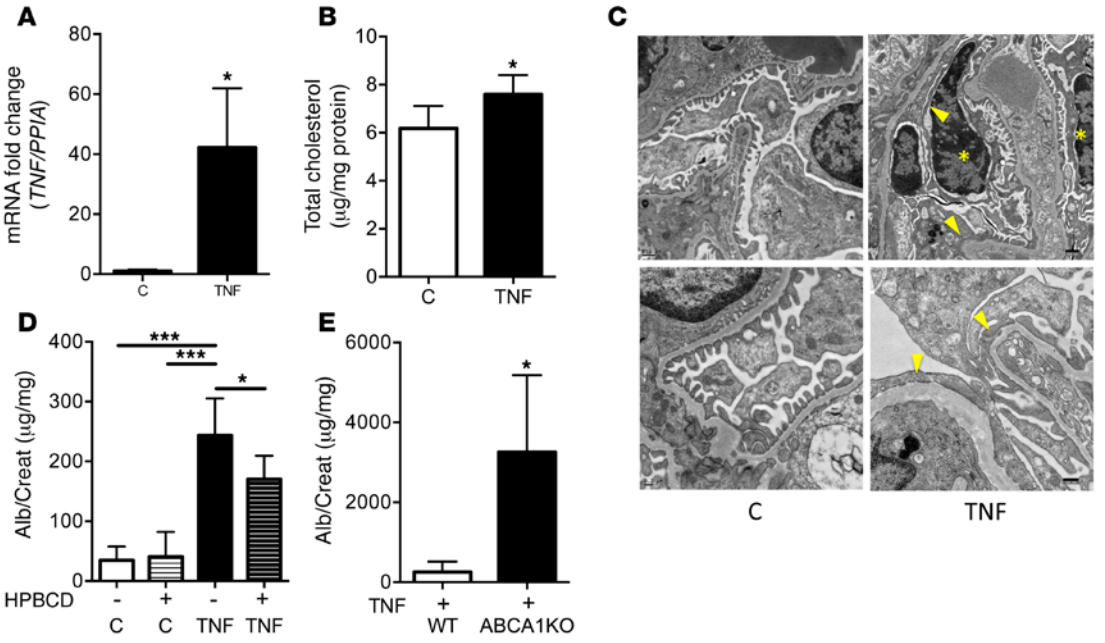

Figure 6. Injection of murine recombinant TNF causes cholesterol-mediated albuminuria. (**A**) Glomerular TNF expression is significantly increased in BALB/cJ mice 6 hours after injection with murine recombinant TNF (TNF) compared with control mice (C) (n = 4 per group). Two-tailed Student's t test; *P < 0.05. (**B**) Bar graph analysis of total cholesterol content in kidney cortexes of TNF-injected mice and in C mice (n = 6 per group). Two-tailed Student's t test; *P < 0.05. (**C**) Transmission electron microscopy analysis of n = 3 mice per group treated with either vehicle (left panels) or TNF (right panels). TNF treatment resulted in segmental foot process effacement (arrowheads) compared with vehicle controls. Focally, podocytes and parietal epithelial cells undergoing apoptosis are detectable, as characterized by condensed chromatin and electron-dense cytoplasm (asterisks) with mitochondrial swelling. Scale bars: 0.5 μm in top panels, 0.2–0.25 μm in bottom panels. (**D**) The urinary albumin-to-creatinine ratio was significantly higher in TNF-injected mice compared with C mice 6 hours after injection. Pretreatment with HPBCD 24 hours before TNF administration significantly reduces albuminuria compared with TNF-treated mice (n = 6 per group). One-way ANOVA; *P < 0.05, ***P < 0.01. (**E**) The urinary albumin-to-creatinine ratio is significantly higher in podocyte-specific ABCA1-deficient mice treated with TNF (KO + TNF) compared with WT mice treated with TNF (WT + TNF) 6 hours after TNF administration (n = 4). Two-tailed Student's t test; *P < 0.05.

cantly reduced in TNF-treated podocytes compared with controls (Figure 4G). As free cholesterol accumulation may be cytotoxic (30–32), we assessed caspase 3 activity as a measure of apoptosis. As shown in Figure 4H, TNF treatment of human podocytes significantly induced apoptosis, which was prevented by depletion of free cholesterol with methyl-β–cyclodextrin (CD). Using the same [^{3}H]-cholesterol labeling assay as described above, we demonstrate that ABCA1OE podocytes were similarly protected from TNF-mediated impairment of cholesterol efflux when compared with empty vector control transfected podocytes (Figure 5A). Additionally, ABCA1OE podocytes were protected from TNF-induced (Figure 5B) and TNFOE-induced (Supplemental Figure 11) apoptosis.

Esterified cholesterol accumulation due to reduced ABCA1-mediated cholesterol efflux is not sufficient to cause podocyte apoptosis. To assess whether decreased ABCA1 expression is sufficient to cause injury, we generated podocytes with knockdown of ABCA1 (siABCA1) (Supplemental Figure 12). Using the [^{3}H]-cholesterol labeling assay described above, we showed that siABCA1 podocytes are characterized by significantly reduced ApoA1-mediated cholesterol efflux compared with scrambled (siCO) control transfected podocytes (Figure 5C). siABCA1 podocytes had increased esterified cholesterol content (Figure 5D) as determined by an enzymatic assay and confirmed by neutral lipid droplet staining with HCS LipidTOX followed by analysis with Opera High Content Screening System. A representative image of the HCS LipidTOX staining and its cell segmentation in Figure 5E shows that siABCA1 had more lipid droplets compared with siCO. Quantitative analysis of images with Acapella Analysis Software revealed a significant increase in the number of neutral lipid droplets per cell in siABCA1 podocytes compared with siCO (Figure 5F). However, the accumulation of esterified cholesterol was not associated with increased podocyte apoptosis (Figure 5H). Overall, these data suggest that decreased ABCA1 expression and esterified cholesterol accumulation per se are not sufficient to cause podocyte apoptosis.

Free cholesterol–mediated apoptosis requires reduced ABCA1-mediated cholesterol efflux in combination with reduced cholesterol esterification activity via SOAT1. Since TNF reduced ABCA1-mediated cholesterol efflux and SOAT1 activity, we investigated whether shifting the balance from esterified to free cholesterol accumulation in siABCA1 podocytes would cause apoptosis. Podocytes were treated with a pharmacological inhibitor of SOAT activity (SI). Quantitative analysis of HCS LipidTOX staining revealed fewer lipid droplets per cell in SI-treated siABCA1 podocytes compared with untreated siABCA1 controls (Figure 5G), suggesting reduced accumulation of esterified cholesterol in the form of lipid droplets. SI treatment did not increase apoptosis in siCO podocytes, whereas it significantly increased apoptosis in siABCA1e podocytes (Figure 5H). These results support a causal role of free rather than esterified cholesterol accu-

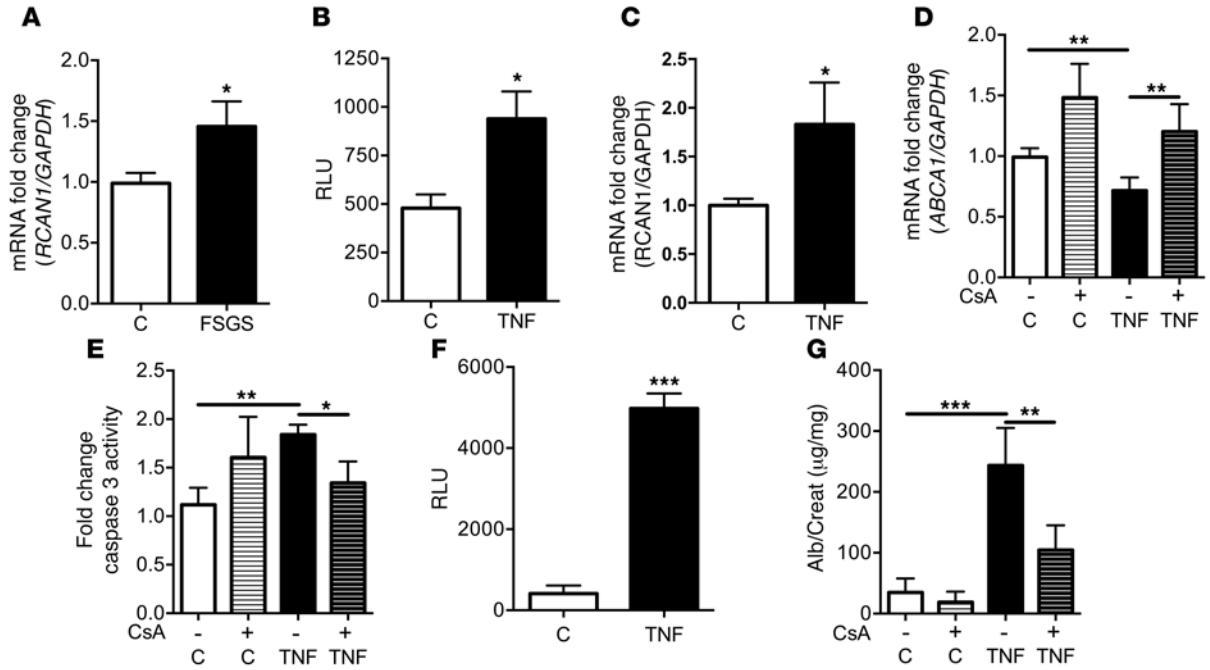

Figure 7. TNF causes NFAT activation and NFAT-mediated ABCA1 repression leading to podocyte apoptosis. (**A**) Quantitative RT-PCR analysis of regulator of calcineurin *1 (RCAN1)* expression in podocytes exposed to sera from individual patients with FSGS ($n = 6$) and healthy patient (C) controls ($n = 3$). One-way ANOVA; $^*P < 0.05$ vs. C. (**B**) TNF increases luciferase activity in mouse podocytes stably transfected with a cDNA coding for the luciferase gene under the control of an NFAT response element compared with untreated controls ($n = 3$). Two-tailed Student's *t* test; $^*P < 0.05$. (**C**) Quantitative RT-PCR analysis of *RCAN1* expression in normal human podocytes exposed to TNF ($n = 3$) shows increased RCAN1 expression in TNF-treated podocytes (TNF) compared with untreated podocytes (C). Two-tailed Student's *t* test; $^*P < 0.05$. (**D**) Quantitative RT-PCR analysis of *ABCA1* expression demonstrating that pretreatment of human podocytes for 1 hour with CsA and continued during TNF treatment (TNF + CsA) prevents TNF-mediated ABCA1 repression compared with TNF-treated cells ($n = 4$). One-way ANOVA; $^{**}P < 0.01$. (**E**) Bar graph analysis showing that pretreatment with CsA and continued during TNF treatment prevents TNF-induced cleaved caspase 3 activity compared with TNF-treated cells ($n = 4$). One-way ANOVA; $^*P < 0.05$, $^{**}P < 0.01$. (**F**) Injection of murine recombinant TNF increases glomerular NFAT-mediated luciferase activity in an NFAT-luciferase reporter mouse model compared with vehicle-treated controls (C) 6 hours after injection ($n = 4$ per group). Two-tailed Student's *t* test; $^{***}P < 0.001$. (**G**) The urinary albumin-to-creatinine ratio was significantly higher in TNF-injected BALB/cJ mice compared with C mice 6 hours after treatment. Pretreatment with CsA 24 hours before TNF administration significantly reduces albuminuria compared with TNF-treated mice ($n = 5$ per group). One-way ANOVA; $^{**}P < 0.01$, $^{***}P < 0.001$.

mulation in podocyte apoptosis and are further strengthened by the observation that free cholesterol depletion with CD prevented SI-induced apoptosis in siABCA1 cells (Figure 5I).

TNF-induced albuminuria in mice is associated with increased kidney cholesterol content and is aggravated in mice with a podocyte-specific Abca1 deletion. To determine whether TNF causes podocyte injury in vivo, 6-week-old BALB/cJ mice were injected i.v. with 0.250 mg/kg of recombinant murine TNF. Glomeruli isolated from these mice showed a significant increase in *Tnf* expression levels (Figure 6A) compared with those from vehicle-treated control mice. Quantitative enzymatic analysis of total cholesterol content in kidney cortex revealed a moderate but significant increase in total cholesterol content in TNF-treated compared with vehicle-treated mice (Figure 6B). Ultrastructural analysis revealed that TNF treatment caused segmental podocyte foot process effacement. Morphological changes including condensation of nuclear chromatin, electron-dense cytoplasm with loss of organelles, and mitochondrial swelling suggesting focal acute injury of a subset of podocytes were observed (Figure 6C). These changes were accompanied by a significant increase in the albumin-to-creatinine ratio 6 hours after TNF injection in comparison with vehicle-injected controls (Figure 6D), but did not result in podocyte loss (Supplemental Figure 13). To investigate whether cholesterol depletion strategies would exert antialbuminuric effects, mice were injected s.c. with 2-hydroxypropyl-β-cyclodextrin (HPBCD) (4,000 mg/kg) as described (17) 18 hours before TNF injection. As expected, cholesterol depletion with Hydroxypropyl-β–cyclodextrin reduced TNF-mediated albuminuria (Figure 6D). In order to further support a link between TNF-induced albuminuria and podocyte ABCA1 expression, we injected recombinant murine TNF into podocyte-specific *Abca1* knockout mice, which did not have albuminuria at baseline (Supplemental Figure 14). Mice were sacrificed 6 hours after TNF administration. At time of sacrifice, podocyte-specific *Abca1* knockout mice had a significantly increased urinary albumin-to-creatinine ratio when compared with controls (Figure 6E). These results indicate that TNF-induced albuminuria is influenced by cholesterol content in podocytes.

TNF-induced NFAT activation in mice results in cholesterol-mediated apoptosis. It was recently described that the proximal promoter region of the *ABCA1* gene has 2 functional NFAT response elements within a 100-bp region upstream of the transcriptional start site that is conserved between mice and humans (23). The functional consequence of this interaction is not well understood. NFAT activation is an important mediator of glomerular damage (33). Since regulator of calcineurin 1 (*RCAN1*)

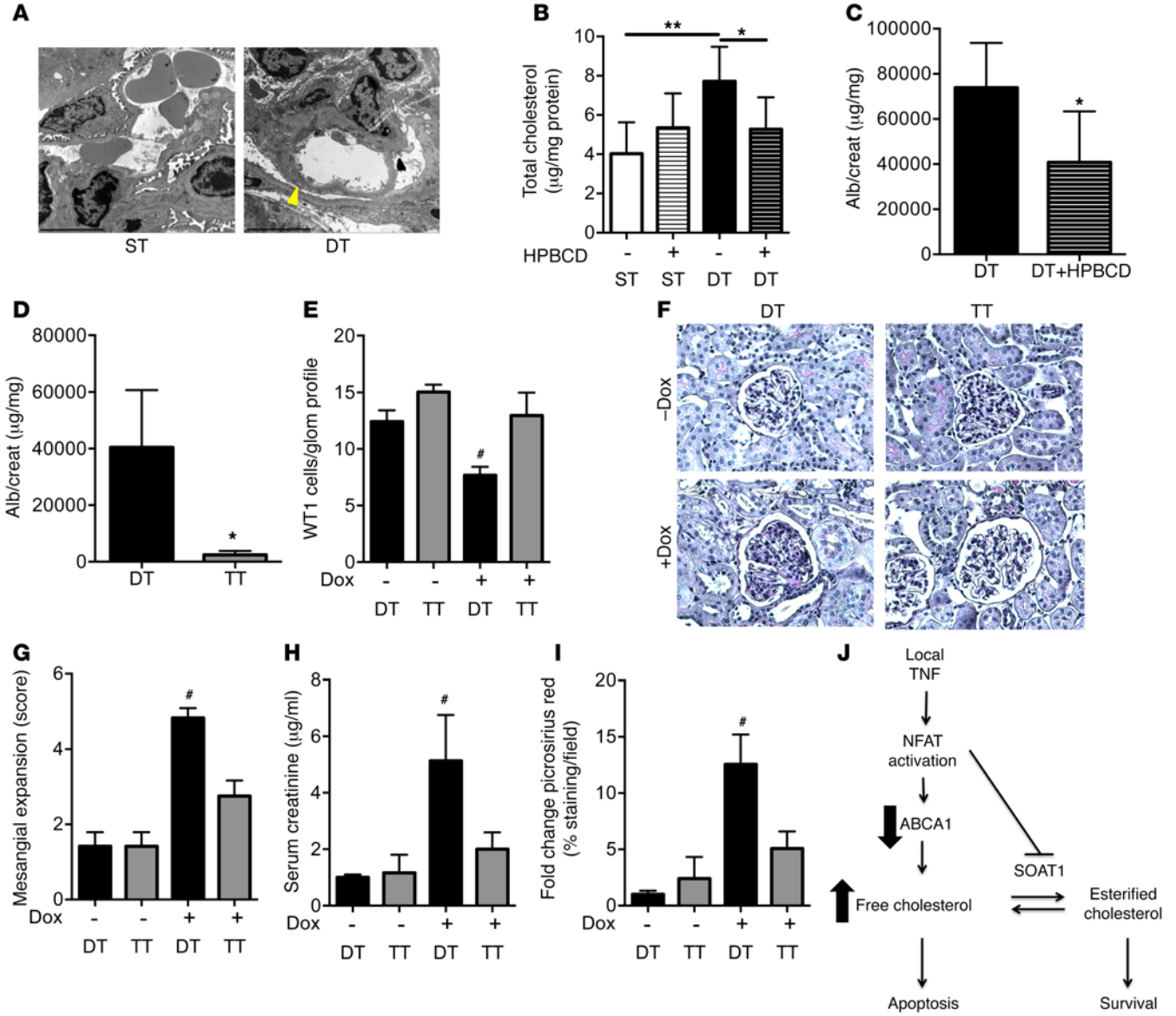

Figure 8. ABCA1 overexpression or treatment with HPBCD can partially prevent NFAT-mediated albuminuria. (**A**) Electron microscopy analysis of double-transgenic (DT) mice fed doxycycline chow for 4 days resulted in segmental foot process effacement (arrowhead) compared with single-transgenic controls (ST). Scale bars: 0.5 μm. (**B**) Total cholesterol content in kidney cortexes of DT and ST mice ($n = 6$ per group) treated with HPBCD or vehicle control. One-way ANOVA; $^{*}P < 0.05$, $^{**}P < 0.01$. (**C**) Urinary albumin-to-creatinine ratio in DT mice treated with HPBCD or vehicle before doxycycline chow feeding ($n = 6$ per group). Two-tailed Student's t test; $^{*}P < 0.05$. (**D**) Urinary albumin-to-creatinine ratio in triple transgenic (TT), inducible podocyte-specific constitutively active NFAT mice overexpressing ABCA1, compared with DT controls after 4 months of doxycycline chow feeding ($n = 3$ per group). Two-tailed Student's t test; $^{*}P < 0.05$. (**E**) Analysis of WT1 podocytes per glomerular profile in DT and TT mice fed control or doxycycline diet for 4 months ($n = 3$). One-way ANOVA; $^{\#}P < 0.05$ compared with all columns. (**F**) Representative periodic acid–Schiff (PAS) staining (original magnification, ×20) of kidney sections from DT and TT mice fed doxycycline or control diet for 4 months. (**G**) Mesangial expansion scores on PAS-stained kidney sections from DT and TT mice fed doxycycline or control diet for 4 months ($n = 3$ per group) as assessed by 2 blinded, independent investigators. One-way ANOVA; $^{\#}P < 0.05$ compared with all columns. (**H**) Bar graph analysis of serum creatinine levels from DT and TT mice fed doxycycline or control diet for 4 months ($n = 3$ per group). One-way ANOVA; $^{\#}P < 0.05$ compared with all columns. (**I**) Bar graph analysis of picrosirius red–stained kidney sections from DT and TT mice fed doxycycline or normal diet ($n = 3$ per group). One-way ANOVA; $^{\#}P < 0.05$ compared with all columns. (**J**) Model of proposed mechanism of local TNF–induced podocyte injury in FSGS and DKD.

expression, a downstream target of NFAT (34), was increased in podocytes exposed to sera from patients with FSGS (Figure 7A), we tested the hypothesis that downregulation of ABCA1 expression by TNF occurs through an NFAT-mediated mechanism. To assess the effect of TNF treatment on NFAT activation, we used a reporter cell line established from mouse podocytes where the luciferase gene is under the control of an NFAT response element (35). Exposure of this cell line to recombinant murine TNF enhanced NFAT promoter activity, leading to increased luciferase activity (Figure 7B) and *RCAN1* expression (Figure 7C), similar to what was observed in TNFOE (Supplemental Figure 15). Finally, to establish a link between TNF-mediated ABCA1 repression and TNF-induced NFAT activation, we treated normal human podocytes with TNF in the presence or absence

of CsA, a known inhibitor of podocyte NFAT activity (22). We observed that TNF-mediated *Abca1* repression (Figure 7D) and induction of apoptosis (Figure 7E) were prevented by CsA.

Systemic TNF administration in mice causes NFAT-mediated albuminuria that can be partially prevented by CsA. To determine whether TNF administration causes NFAT activation in vivo, we used a transgenic reporter mouse model expressing luciferase under the control of nine NFAT response elements from the IL-4 promoter (36). Following i.v. TNF injection, glomeruli were isolated and luciferase activity was assessed after 6 hours. TNF-treated mice showed increased glomerular luciferase activity compared with vehicle-treated controls (Figure 7F). Although systemic TNF administration may impose off-target effects, our data confirm an effect of TNF on the glomerulus and support a direct effect on podocytes.

To determine whether pharmacological inhibition of calcineurin and downstream NFAT signaling could prevent TNF-induced albuminuria, CsA was administered orally (50 mg/kg) to 6-week-old BALB/cJ mice 18 hours before TNF administration. As in our previous experiments, TNF administration caused significant albuminuria 6 hours after injection, which was partially prevented by CsA (Figure 7G).

Taken together, these results support a role for podocyte NFAT activation in TNF-induced albuminuria.

Podocyte-specific NFAT activation causes albuminuria that can be attenuated by HPBCD. Our in vitro experiments suggested that NFAT activation causes podocyte injury by altering cholesterol homeostasis in an ABCA1-dependent manner. To confirm these observations in vivo, we used a transgenic mouse model with podocyte-specific inducible (*podocin-rt-TA*) overexpression of constitutively active NFATc1 (*Nfatc1^{nuc}*). The *Nfatc1^{nuc}* transgene was generated by mutation of the *Nfatc1* gene at 21 positions, leading to the substitution of alanine residues for serine (37). *Nfatc1^{nuc}* mice were previously reported to develop albuminuria 4 days after induction of *Nfatc1^{nuc}* (DT) expression by doxycycline compared with single-transgenic controls (ST) (35). In fact, electron microscopy analysis revealed podocyte foot process effacement in DT mice compared with ST controls (Figure 8A) but no histological changes by light microscopy analysis of H&E staining (Supplemental Figure 16). To examine the role of altered podocyte cholesterol homeostasis in NFAT-mediated podocyte injury, 6-week-old *Nfatc1^{nuc}* mice were fed doxycycline chow for 4 days, and cholesterol content in the kidney cortex was analyzed. DT mice showed significantly increased cholesterol content (Figure 8B) in the kidney cortex compared with ST controls. As expected, DT mice developed albuminuria, which was partially prevented by administration of HPBCD (Figure 8C). These results support a causative role of kidney cholesterol accumulation in the development of NFAT-mediated albuminuria. In order to confirm that NFAT-mediated albuminuria is ABCA1 dependent, we performed a rescue experiment and generated triple-transgenic mice with podocyte-specific *Nfatc1^{nuc}* activation and glomerular *Abca1* overexpression (TT), which were fed doxycycline chow for 4 months. Our data demonstrated that NFAT-mediated albuminuria (Figure 8D) and podocyte loss (Figure 8E) can be prevented in TT mice. Additionally, TT mice were protected from mesangial expansion (Figure 8, F and G), elevated serum creatinine (Figure 8H), and increased picrosirius red staining (Figure 8I). These data strongly support that NFAT activation plays a causal role in ABCA1-dependent cholesterol accumulation leading to podocyte injury and the development of albuminuria.

Discussion

Our study provides several novel findings. First, we demonstrate the dissociation between systemic and local TNF pathway activation in the pathogenesis of podocyte injury. These findings challenge the translatability of systemic TNFR1 and TNFR2 from their strong role as biomarkers to a potential role as therapeutic targets. Second, we have used a unique translational approach combining clinical and experimental research to dissect the causal role of glomerular TNF expression in podocyte injury in DKD and FSGS, which are discordant in the level of circulating TNF. Third, we describe for the first time to our knowledge the opposing roles of free (proapoptotic) and esterified cholesterol (antiapoptotic) as key mediators of TNF-induced podocyte injury. Fourth, we describe the mechanism linking TNF to podocyte injury via modulation of ABCA1 and SOAT1 function. Finally, we identify NFATc1 activation as the link between TNF and ABCA1 repression, thus shedding new light on the mechanism of TNF-induced local injury in glomerular diseases as well as other chronic inflammatory conditions.

Although CKD per se is considered a chronic inflammatory disorder (38), the contribution of inflammatory mediators to kidney damage remains largely unknown. Recent studies have identified increased serum TNF, TNFR1, and TNFR2 to predict the progression of DKD (9, 10, 12), but a causal role of these cytokines in the development and/or progression of DKD has not been established. Our data indicate that TNF but not TNFR1 or TNFR2 causes podocyte apoptosis (Figure 3G). Furthermore, as podocytes exposed to DKD and FSGS sera show increased local TNF expression, and TNF inhibition prevents patient sera–mediated podocyte apoptosis (Figures 2 And 3) irrespectively of serum TNF levels, our data support the importance of locally expressed TNF as a major driver of podocyte injury. In fact, elevated local TNF expression was shown to reflect disease severity better than systemic TNF levels in several inflammatory diseases (39, 40), and reduced renal TNF expression was shown to correlate with reduced albuminuria independently of serum TNF levels in mice (41). This supports that circulating TNFR1/TNFR2 may represent a compensatory mechanism to elevated local TNF. Further supporting the role for local TNF expression, it was shown that TNF inhibitors demonstrate efficacy in a subset of patients with FSGS enrolled in the FONT Study (14, 42) in the absence of evidence of elevated serum TNF levels in these patients. These observations are consistent with our prior findings that local factors such as sphingolipid-related enzymes are a key mediator of danger signaling in podocytes irrespectively of the level of circulating factors (43). Taken together, these observations support a causative role for local TNF expression in the development of kidney disease and more broadly in peripheral cell injury.

Although we do not identify the specific stimuli that increase local TNF expression in FSGS and DKD, it is interesting that exogenous TNF is sufficient to induce local TNF expression in podocytes. This suggests that circulating TNF in DKD but not in FSGS may at least in part contribute to increased glomerular TNF

expression. The potential circulating factors in FSGS that may affect glomerular TNF expression remain to be identified. While soluble urokinase-type plasminogen activator receptor (suPAR) correlates with circulating TNF in lupus erythematosus (44) and causes podocyte injury in FSGS (45), the ability of circulating suPAR to affect local TNF expression remains to be established. Similarly, it would be interesting to determine whether circulating autoantibodies including anti-CD40 (46) or cytokine receptor–like factor-1 (CRLF-1) (47), which are linked to proteinuria in FSGS, may cause TNF-mediated podocyte injury. Additionally, the TLR4 ligand lipopolysaccharide, which causes acute podocyte injury and is elevated in sera from patients with DKD (48, 49), is also necessary for trafficking of TNF to the plasma membrane (50). Finally, the possibility that other local factors contribute to TNF pathway activation in podocytes exposed to patient sera should also be considered. Therefore, it is likely that a combination of local and systemic factors may contribute to modulation of local TNF pathway activation, irrespectively of circulating TNF.

Recent experimental evidence suggests that local TNF causes inflammasome activation (51) and is associated with altered cholesterol homeostasis (52). Our clinical observations demonstrate that increased glomerular *TNF* expression in patients with FSGS correlates with reduced eGFR in the NEPTUNE cohort (Figure 3D) and with reduced ABCA1 expression in the ERCB cohort (Supplemental Figure 9), suggesting a role of local TNF in the pathogenesis of glomerular diseases. The ability of TNF to inhibit ABCA1 expression and function in podocytes (Figure 4) may be cell-type specific, as in macrophages TNF expression positively correlates with ABCA1 expression and ABCA1-mediated cholesterol efflux (27). While TNF causes NF-κB activation in Caco-2 cells and macrophages, the discrepant effect of TNF on ABCA1 expression (upregulated in macrophages and downregulated in Caco-2) suggests that mechanisms other than NF-κB may modulate ABCA1 expression (53). In fact, p38 has been described as a key mediator linking TNF to increased ABCA1 expression in macrophages (54). Therefore, it seems possible that TNF signals primarily through p38 in macrophages or that macrophages and podocytes express different p38 isoforms leading to converse effects on ABCA1 transcription (55).

Since knockdown of ABCA1 did not lead to podocyte injury in vitro (Figure 5) and in vivo (Supplemental Figure 14), it is likely that a second hit is required to cause podocyte injury. In fact, while reduced ABCA1 expression alone is not sufficient to cause podocyte injury, simultaneous pharmacological inhibition of the conversion of free cholesterol to esterified cholesterol in ABCA1 knockdown podocytes was sufficient to cause cell injury (Figure 5). In further support of this second-hit model, our in vivo data demonstrate that while *Abca1* knockout mice are not albuminuric at baseline, they are more susceptible to TNF-induced albuminuria (Figure 6). However, the highly complex nature of cholesterol-mediated cell injury in vivo requires further investigation, as other studies yielded conflicting results showing either protective or detrimental effects of esterified cholesterol accumulation in atherosclerotic phenotypes (56). Our data suggest that, in podocytes, irrespectively of the amount of esterified cholesterol that accumulates, cell injury is mainly caused by free cholesterol. While SOAT1 activity is likely to be tightly regulated to maintain cholesterol homeostasis in normal podocytes, the possibility that altered SOAT1 activity contributes to podocyte injury in disease conditions warrants further investigation. It would be interesting to determine whether TNF-induced podocyte injury is linked to the formation of cholesterol crystals, a phenomenon that was recently shown to be prevented by HPBCD in macrophages in the setting of atherosclerosis (57).

Our data also support a role for TNF in activating NFAT signaling leading to altered cholesterol metabolism via reduced ABCA1 expression, thus contributing to kidney injury. Although inhibition of NFAT with CsA may directly rescue podocyte dysfunction in glomerular injury (22), long-term treatment with calcineurin inhibitors is associated with significant toxicity (58). Thus, the identification of new downstream targets of NFAT activation in podocytes is crucial to the development of new therapeutic strategies. Interestingly, 4-day feeding of doxycycline chow in DT (podocyte-specific constitutively active *Nfatc1*^{nuc}) mice is characterized by altered cholesterol homeostasis, podocyte foot process effacement, and albuminuria that can be partially prevented by cholesterol depletion (Figure 8). On the contrary, *Nfatc1*^{nuc} mice (DT) fed doxycycline chow for 4 months developed podocyte loss, glomerulosclerosis, elevated serum creatinine, and increased collagen staining. Overexpression of ABCA1 in *Nfatc1*^{nuc} mice (TT) was sufficient to prevent this CKD-like phenotype. As our short-term and long-term mouse models demonstrate efficacy of HPBCD and ABCA1 overexpression, it seems feasible to propose that HPBCD or drugs that increase ABCA1-mediated cholesterol efflux may represent a new class of drugs to treat patients affected by proteinuric glomerular disorders. Our data also suggest that cholesterol-targeted therapies may have a beneficial effect in diseases of nonglomerular origin that respond to CsA treatment, such as rheumatoid arthritis or psoriasis. Further investigations are required to understand whether agents facilitating podocyte cholesterol efflux maintains their beneficial effects in the setting of established CKD.

In conclusion, our results uncover a novel mechanism where cholesterol-mediated podocyte injury is the result of increased endogenous *TNF* expression, thus possibly contributing to the development of FSGS and DKD. To our knowledge, this is the first study showing that local TNF contributes to lipid-mediated podocyte injury in FSGS and DKD by a dual mechanism that requires both reduced ABCA1 expression and reduced SOAT1 activity. The fact that this occurs irrespectively of sera TNF levels challenges the idea of using circulating TNF, TNFR1, and TNFR2 for the implementation of patient-specific targeted therapies. We also demonstrate a novel role for NFAT as a downstream target of TNF in podocytes. NFAT acts as a transcriptional repressor of ABCA1 expression, and overexpression of ABCA1 is sufficient to prevent NFAT-induced podocyte injury and albuminuria, providing the rationale to study agents targeting cholesterol efflux in proteinuric kidney diseases. Additional studies are needed to investigate the role of TNF- or NFAT-mediated dysregulation of cholesterol homeostasis in the context of nonglomerular diseases.

Methods

Study approval. All study protocols involving mice were approved by the University of Miami's IACUC (Miami, FL, 2016). The University of Miami (UM) has an Animal Welfare Assurance on file with the Office

of Laboratory Animal Welfare, NIH (A-3224-01, effective November 24, 2015). Additionally, UM is registered with the US Department of Agriculture Animal and Plant Health Inspection Service, effective December 2014, registration 58-R-007. As of October 22, 2013, the Council on Accreditation of the Association for Assessment and Accreditation of Laboratory Animal Care (AAALAC International) has continued UM's full accreditation. All study protocols involving human samples were granted IRB exemption since the samples were collected under an IRB-approved research study for which informed consent was obtained and there was no access to identifiable information (Human Subjects Research Office, Miami, FL, 2012, and Human Research Protection Program, Ann Arbor, MI, 2015). Appropriate safeguards were in place to protect subject confidentiality and privacy.

Analysis of patient sera and kidney biopsies. Three cohorts were used for this study: (a) serum samples from 10 healthy controls, 10 patients with T1D, and 10 patients with T1D and kidney disease from the Finnish Diabetic Nephropathy (FinnDiane) Study (17); (b) 14 serum samples from patients with steroid-dependent NS (Supplemental Table 1); and (c) 6 serum samples from patients with biopsy-proven FSGS (59). Serum TNF, TNFR1, and TNFR2 were measured according to the manufacturer's instructions (Quantikine HS ELISA human TNF-α, Quantikine ELISA human TNF-RII/TNFRSF1B, and Quantikine ELISA human sTNFRI/TNFRSF1A; R&D Systems) or Luminex Assay (Eve Technologies, Canada) using previously described methods (60). For glomerular expression, kidney biopsy specimens from patients with minimal-change disease (n = 24), and patients with FSGS (n = 14) were obtained from the ERCB, and specimens from minimal-change disease patients (n = 42) and FSGS patients (n = 48) were obtained from the Nephrotic Syndrome Study Network (NEPTUNE). Biopsy samples represent those that were available for expression analysis and that passed quality control measures at the time of study. ERCB and NEPTUNE gene expression data were normalized and quantified on a probeset level using custom CDF annotations on Affymetrix U133 and Affymetrix ST 2.1 platforms, respectively, as previously described (26, 61).

Podocyte culture. Human podocytes were cultured as previously described (62). Briefly, podocytes were grown under permissive conditions at 33°C temperature in media containing 0.01 mg/ml recombinant human insulin, 0.0055 mg/ml human transferrin (substantially iron-free), and 0.005 μg/ml sodium selenite, then thermoshifted to 37°C and differentiated for 14 days. Stable podocyte cell lines expressing siABCA1 or nontargeting siRNA (Applied Biological Materials) were developed by lentiviral infection. Clones were obtained by limited dilution and expanded under puromycin selection. *ABCA1* knockdown in different clones was confirmed by Western blotting and analysis of ABCA1-mediated cholesterol efflux. The clone with the most efficient knockdown for *ABCA1* was chosen for further experiments. A stable cell line expressing GFP-labeled ABCA1 (63) (vector gift from Michael Fitzgerald) or GFP alone was developed by transfection with Fugene (Promega) followed by cell sorting. A stable cell line expressing siTNF (Applied Biological Materials) was developed by lentiviral infections followed by puromycin selection.

Differentiated podocytes were serum restricted for 24 hours before treatments. For pharmacological inhibition experiments, podocytes were treated for 1 hour with cyclosporin A (CsA, 0.1 μg/ml; Sigma-Aldrich), methyl-β–cyclodextrin (CD, 5 mmol/l; Sigma-Aldrich), TNFR2 (R2B, 3 μg/ml; R&D Systems), or TNFR1 antibody (R1B, 10 μg/ml; Santa Cruz Biotechnology) where indicated, followed by treatment with recombinant human TNF (100 ng/ml; R&D Systems), recombinant human TNFR1 or TNFR (125 ng/ml; R&D Systems), Sandoz 58-032 (SI, 4 μM; Sigma-Aldrich), empty vector or TNF-overexpressing lentivirus (Origene), or 4% patient sera for 24 hours. Some experiments were completed with pooled patient sera as indicated. Podocytes were analyzed as described below.

Apoptosis analysis. Apoptosis was assessed using the Caspase-3 Fluometric HTS Assay Kit (Biotium) or ApoTox-Glo Triplex Assay (Promega) according to the manufacturer's instructions. Briefly, differentiated podocytes were treated as indicated, and caspase 3 activity was determined after 2 hours at excitation 470 nm, emission 520 nm for the former, or excitation 400 nm, emission 505 nm for viability and luminescence for 1 second for caspase 3 activity for the latter. Additionally, cytotoxicity was measured using the ApoTox-Glo Triplex Assay according to the manufacturer's instructions, with excitation 485 nm and emission 520 nm. Values were expressed as fold change in comparison with controls.

Cholesterol efflux and SOAT activity assays. To measure cholesterol efflux from differentiated human podocytes, a previously described method was performed with some modifications (64). Podocytes were labeled with 1 μCi/ml [^{3}H]-cholesterol in medium with 2% FBS for 16 hours; cells were washed with PBS and then incubated in RPMI containing 10 μg/ml ApoA1 (Millipore) for 6 hours. An aliquot of medium was recovered for measurement of radioactivity by scintillation counting. Podocytes were washed twice with PBS, followed by cellular lipid extraction with hexane/isopropanol 3:2 (vol/vol). Lipids were separated by thin-layer chromatography in heptane/diethylether/methanol/acetic acid 80:30:3:1.5 (vol/vol/vol/vol) to quantify free and esterified cholesterol radioactivity by scintillation counting. Cellular proteins were dissolved in 0.1% SDS in 0.1 M NaOH and quantified by bicinchoninic acid assay (BCA assay) method. Cholesterol efflux to medium containing serum was expressed as percentage of total cell cholesterol by scintillation counting as previously described (65).

Esterification of cellular cholesterol by SOAT was measured as previously described with modifications (64). Differentiated podocytes were incubated with 2 μCi/ml [^{14}C]-oleate for 1 hour at 37°C. Cellular lipids were extracted and separated by thin-layer chromatography (TLC) as described above, followed by scintillation counting.

Determination of cholesterol mass. To determine total cholesterol mass, differentiated podocytes were grown in 100-mm plates. Cellular lipids were extracted as described above. Total cholesterol content was measured using the Amplex Red Cholesterol Assay Kit (Invitrogen) following manufacturer instructions and normalized to cell protein content using the BCA method.

To determine esterified cholesterol content, differentiated podocytes were grown in 100-mm plates. Cellular lipids were extracted and lipids were separated by TLC as described above. Esterified cholesterol was re-extracted from the TLC plates with chloroform and evaporated under a stream of N_2 gas. Esterified cholesterol was determined by enzymatic conversion to free cholesterol using the Amplex Red Cholesterol Assay Kit (Invitrogen).

High-content lipid droplet quantification. Following treatment, differentiated podocytes were fixed with 4% paraformaldehyde/sucrose. Cells were stained with HCS LipidTOX Red (Invitrogen) and HCS CellMask Blue (Invitrogen) according to the manufacturer's instructions. Cells were imaged by the Opera High Content Screening

System using the ×20 confocal lens. Acapella High Content Imaging and Analysis software (PerkinElmer) was used for analysis. Nuclei and cellular segmentation was detected using standard detection modules in the UV channel. Within the detected cytoplasm region, neutral lipid droplets were detected in the red fluorescence channel using intensity thresholds. From the cell segmentation and lipid droplet images, the number of lipid droplets per cell was determined with analysis of more than 300 cells per well.

Quantitative real-time PCR. RNA was extracted from differentiated podocytes using the RNeasy Mini Kit (Qiagen). Reverse transcription was performed using qScript cDNA SuperMix (Quanta) according to the manufacturer's protocols. Quantitative real-time PCR (RT-PCR) was performed using the StepOnePlus system (Applied Biosystems) with PerfeCTA SYBR Green FastMix (Quanta) using the ΔΔct method.

Western blot analysis. Cell lysis was performed with 3-[(3-cholamidopropyl)dimethylammonio]-1-propanesulfonic (CHAPS) acid buffer. Western blot analysis was performed as previously described (59) using the following primary antibodies: anti-GAPDH (cb1001, 1:10,000; Calbiochem), anti-ABCA1 (ab18180, 1:1,000; Abcam), or anti-TNF (6945, 1:1,000; Cell Signaling); or the following secondary antibodies: anti-mouse IgG HRP (W402B, 1:10,000; Promega) or anti-rabbit IgG HRP (W401B, 1:10,000; Promega).

Luciferase assay. NFAT reporter podocyte cell lines were previously generated (35). Briefly, mouse podocytes that stably express the pGL4.30 reporter plasmid (Promega) with *luc*2P firefly luciferase gene under the control of the NFAT response element were generated by hygromycin selection. Podocytes were differentiated for 14 days and treated as described above. Cells were lysed using the Bright-Glo Luciferase Assay System (Promega), and luminescence was measured on a SpectraMax L microplate reader (Molecular Devices) and normalized to protein content by NanoOrange Protein Quantification Kit (Invitrogen) using the manufacturer's instructions with slight modifications.

Animal studies. Thirty-six female mice (BALB/cJ, stock number 000651) at the age of 5–6 weeks were purchased from Jackson Laboratory. Mice were treated with pharmacological agents as indicated 24 hours before TNF treatment. Pharmacological agents were used at the following concentrations: hydroxypropyl-beta-cyclodextrin (HPBCD), 4,000 mg/kg, s.c. (Sigma-Aldrich); CsA, 50 mg/kg, orally (Teva). Recombinant murine TNF was used (0.25 mg/kg, tail vein injection; Biolegend). Spot urine was collected before sacrifice and 6 hours after TNF injection.

Podocyte-specific *Abca1*$^{fl/fl}$ (*Abca1* knockout) mice were generated by crossing of floxed *Abca1* mice (66) (gift from John Parks) to *podocin-Cre* mice [B6.Cg-Tg(NPHS2-cre)295Lbh/J, #008205]. Albuminuria was induced by injection of murine recombinant TNF in 5- to 6-week-old females as described above. Spot urine was collected before sacrifice and 6 hours after TNF injection.

Mice with constitutive expression of luciferase under control of an *NFAT* response element (36) [FVB-Tg(Myh6/NFAT-luc)1Jmol/J, #010588] were purchased from Jackson Laboratory and expanded. At 6 weeks of age, female mice were injected with murine recombinant TNF (Biolegend) as described above. Glomeruli were isolated and measurement of luciferase activity was determined as described above.

Inducible constitutively active *Nfatc1* transgenic mice (*Nfatc1*^{nuc}) were a gift from Gerald R. Crabtree (B6BAF1/J). These mice were bred to *podocin*-reverse tetracycline-controlled transactivator, *podocin-rt-TA* mice [FVB/N-Tg(NPHS2-rtTA2*M2)1Jbk/J, #008202; Jackson Laboratory] to generate double-transgenic podocyte-specific tetracycline-inducible constitutively active NFATc1 mice (DT). The colony was maintained in the F_1 generation. At 5–6 weeks of age, mice were injected with HPBCD (4,000 mg/kg, s.c.). Twenty-four hours later, *Nfatc1*^{nuc} expression was induced by doxycycline chow feeding (2,000 ppm) for 4 days. Additional CD boluses were given every other day. Mice were sacrificed after 4 days, and phenotypic analysis was performed. An additional group of DT mice was crossed to *Abca1* transgenic mice [B6.Cg-Tg(Prnp-Abca1)Ehol/J, #008596] purchased from Jackson Laboratory to generate triple-transgenic, ABCA1-overexpressing, podocyte-specific tetracycline-inducible constitutively active NFATc1 mice (TT). N1 mice were fed doxycycline chow to induce *NFATc1*^{nuc} expression for 4 months. Spot urine, sera, and kidney tissue for histological analysis were collected at time of sacrifice.

Phenotypic analysis of mice. At baseline and at time of sacrifice, spot urine was collected and urinary albumin-to-creatinine ratios were determined using an ELISA (Bethyl Laboratories) for albumin detection and a biochemical assay based on the Jaffe method for creatinine detection (Stanbio). All albuminuria values are expressed as micrograms albumin per milligram creatinine. Serum creatinine was determined by tandem mass spectrometry at the University of Alabama at Birmingham–UCSD O'Brien Core Center.

At sacrifice, isotonic saline perfusion was performed. The left kidney was used for isolation of glomeruli for mRNA analysis by sieving method (17). The right kidney was removed for cholesterol content determination. Extraction of mRNA was performed using QIAzol (Qiagen) according to the manufacturer's instructions. Determination of cholesterol content in kidney cortex was determined in snap-frozen tissue by homogenization in 2 mM potassium phosphate buffer. Samples were extracted 2 times for 30 minutes in hexane/isopropanol (3:1) on a shaker. Hexane/isopropanol residues were evaporated using a SpeedVac (Centrivap DNA concentrator, Lab Conco). Samples were reconstituted in assay buffer, and total cholesterol content was quantified with the Amplex Red Cholesterol Assay Kit (Invitrogen) according to the manufacturer's instructions. Kidney cortex pellets were homogenized in 0.1 M NaOH/0.1% SDS, and protein content was quantified for normalization by BCA method.

For electron microscopy, animals were perfused with 4% paraformaldehyde, 1% glutaraldehyde in 0.1 M phosphate buffer (pH 7.4) for 3 minutes at 3 ml/min. The solution was exchanged after 24 hours, before embedding. Picrosirius red, H&E, and periodic acid–Schiff (PAS) staining of 4-μm-thick kidney sections was performed as previously described with slight modifications (17, 67). Picrosirius red was visualized by polarized light microscopy followed by analysis with ImageJ. Twenty glomeruli per section were analyzed for mesangial expansion by semiquantitative analysis (scale 0–5) performed by 2 blinded independent investigators on PAS-stained sections. To determine podocyte numbers per glomerular profile, we adapted the method as previously described (68). Four-micrometer-thick tissue sections were stained with anti-WT1 antibody (1:200; Santa Cruz Biotechnology).

Statistics. All values are represented as means with SD. Statistical analysis was performed using Prism GraphPad 6 software. Results were analyzed using 1-way ANOVA. When 1-way ANOVA showed statistical significance, results were compared using a 2-tailed Student's *t* test after Tukey's correction for multiple comparisons. A *P* value less than 0.05 was considered statistically significant.

Author contributions

CEP conceived the project, performed the in vitro and in vivo experiments, analyzed the data, and wrote the manuscript. FL, GMD, JM-D, AM, MG, TH, OK, and TH performed some of the in vitro and in vivo experiments. ML, MIL, C. Forsblom, HR, and P-HG collected patient samples and clinical information and performed some of the experiments involving the analysis of patient samples. AJM designed and performed experiments related to cholesterol determination and cholesterol efflux. C. Faul and AS provided models and expertise for in vivo experiments. GWB conceived 1 of the techniques used. S. Merscher and AF conceived the project, designed and supervised the study, analyzed the data, and edited the manuscript. S. Martini analyzed glomerular expression data available from the European Renal cDNA Bank (ERCB). AF is the guarantor of this work and, as such, had full access to all the data in the study and takes responsibility for the integrity of the data and the accuracy of the data analysis.

Acknowledgments

AF is supported by NIH grants R01DK090316, R01DK104753, U-24-DK076169, U-54-DK083912, U-M1-DK100846, and 1U-L1-TR000460. AF, S. Merscher, and C. Faul are supported by Hoffman-La Roche. CP is supported by American Heart Association predoctoral fellowship 14PRE20380743. C. Faul is supported by grant R01HL128714 from the NIH. The study was also supported by the Folkhälsan Research Foundation (P-HG), the Wilhelm and Else Stockmann Foundation (P-HG, MIL, ML), the Liv och Hälsa Foundation (P-HG, MIL), Waldemar von Frenckells stiftelse (MIL), Kyllikki ja Uolevi Lehikoinen Foundation (MIL), Svenska Kulturfonden (MIL), Academy of Finland (P-HG), the Novo Nordisk Foundation (P-HG, NNF14SA0003), and the Diabetes Research Foundation (ML). We thank nurses Anna Sandelin, Jaana Tuomikangas, and Tuula Soppela at the Folkhälsan Institute of Genetics for technical assistance. The Nephrotic Syndrome Study Network Consortium (NEPTUNE), U54-DK-083912, is a part of the NIH Rare Disease Clinical Research Network, supported through a collaboration between the Office of Rare Diseases Research, the National Center for Advancing Translational Sciences, and the National Institute of Diabetes and Digestive and Kidney Diseases. Additional funding and/or programmatic support for this project has also been provided by the University of Michigan, NephCure Kidney International, and the Halpin Foundation. This study was further supported by the German Research Foundation (CRC 1140, CRC 992, and Heisenberg program to TBH), by the European Research Council (ERC grant to TBH), and by the Excellence Initiative of the German Federal and State Governments (BIOSS to TBH). A special thanks to the Katz Family naming the center where these studies were conducted.

Address correspondence to: Alessia Fornoni or Sandra Merscher, Division of Nephrology and Hypertension and Peggy and Harold Katz Drug Discovery Center, University of Miami Miller School of Medicine, 1580 NW 10th Avenue, Miami, Florida 33136, USA. Phone: 305.243.3583; E-mail: afornoni@med.miami.edu (A. Fornoni). Phone: 305.243.6558; E-mail: smerscher@med.miami.edu (S. Merscher).

1. Scott DL, Kingsley GH. Tumor necrosis factor inhibitors for rheumatoid arthritis. *N Engl J Med*. 2006;355(7):704–712.
2. Selmaj K, Raine CS, Cannella B, Brosnan CF. Identification of lymphotoxin and tumor necrosis factor in multiple sclerosis lesions. *J Clin Invest*. 1991;87(3):949–954.
3. McKellar GE, McCarey DW, Sattar N, McInnes IB. Role for TNF in atherosclerosis? Lessons from autoimmune disease. *Nat Rev Cardiol*. 2009;6(6):410–417.
4. Vincent FB, Morand EF, Murphy K, Mackay F, Mariette X, Marcelli C. Antidrug antibodies (ADAb) to tumour necrosis factor (TNF)-specific neutralising agents in chronic inflammatory diseases: a real issue, a clinical perspective. *Ann Rheum Dis*. 2013;72(2):165–178.
5. Johnson AM, Olefsky JM. The origins and drivers of insulin resistance. *Cell*. 2013;152(4):673–684.
6. Navarro JF, Mora C, Maca M, Garca J. Inflammatory parameters are independently associated with urinary albumin in type 2 diabetes mellitus. *Am J Kidney Dis*. 2003;42(1):53–61.
7. Moriwaki Y, et al. Elevated levels of interleukin-18 and tumor necrosis factor-alpha in serum of patients with type 2 diabetes mellitus: relationship with diabetic nephropathy. *Metab Clin Exp*. 2003;52(5):605–608.
8. Pavkov ME, et al. Tumor necrosis factor receptors 1 and 2 are associated with early glomerular lesions in type 2 diabetes. *Kidney Int*. 2016;89(1):226–234.
9. Gohda T, et al. Circulating TNF receptors 1 and 2 predict stage 3 CKD in type 1 diabetes. *J Am Soc Nephrol*. 2012;23(3):516–524.
10. Niewczas MA, et al. Circulating TNF receptors 1 and 2 predict ESRD in type 2 diabetes. *J Am Soc Nephrol*. 2012;23(3):507–515.
11. Forsblom C, et al. Added value of soluble tumor necrosis factor-α receptor 1 as a biomarker of ESRD risk in patients with type 1 diabetes. *Diabetes Care*. 2014;37(8):2334–2342.
12. Pavkov ME, Nelson RG, Knowler WC, Cheng Y, Krolewski AS, Niewczas MA. Elevation of circulating TNF receptors 1 and 2 increases the risk of end-stage renal disease in American Indians with type 2 diabetes. *Kidney Int*. 2015;87(4):812–819.
13. Peyser A, et al. Follow-up of phase I trial of adalimumab and rosiglitazone in FSGS: III. Report of the FONT study group. *BMC Nephrol*. 2010;11:2.
14. Joy MS, et al. Phase 1 trial of adalimumab in Focal Segmental Glomerulosclerosis (FSGS): II. Report of the FONT (Novel Therapies for Resistant FSGS) study group. *Am J Kidney Dis*. 2010;55(1):50–60.
15. Rohatgi A, et al. HDL cholesterol efflux capacity and incident cardiovascular events. *N Engl J Med*. 2014;371(25):2383–2393.
16. Fornoni A, Merscher S, Kopp JB. Lipid biology of the podocyte — new perspectives offer new opportunities. *Nat Rev Nephrol*. 2014;10(7):379–388.
17. Merscher-Gomez S, et al. Cyclodextrin protects podocytes in diabetic kidney disease. *Diabetes*. 2013;62(11):3817–3827.
18. Herman-Edelstein M, Scherzer P, Tobar A, Levi M, Gafter U. Altered renal lipid metabolism and renal lipid accumulation in human diabetic nephropathy. *J Lipid Res*. 2014;55(3):561–572.
19. Cattran DC, et al. Cyclosporin in idiopathic glomerular disease associated with the nephrotic syndrome : workshop recommendations. *Kidney Int*. 2007;72(12):1429–1447.
20. Flanagan WM, Corthésy B, Bram RJ, Crabtree GR. Nuclear association of a T-cell transcription factor blocked by FK-506 and cyclosporin A. *Nature*. 1991;352(6338):803–807.
21. Gómez-Sintes R, Lucas JJ. NFAT/Fas signaling mediates the neuronal apoptosis and motor side effects of GSK-3 inhibition in a mouse model of lithium therapy. *J Clin Invest*. 2010;120(7):2432–2445.
22. Faul C, et al. The actin cytoskeleton of kidney podocytes is a direct target of the antiproteinuric effect of cyclosporine A. *Nat Med*. 2008;14(9):931–938.
23. Maitra U, Parks JS, Li L. An innate immunity signaling process suppresses macrophage ABCA1 expression through IRAK-1-mediated down-regulation of retinoic acid receptor alpha and NFAT*c2*. *Mol Cell Biol*. 2009;29(22):5989–5997.
24. Martini S, et al. Integrative biology identifies shared transcriptional networks in CKD. *J Am Soc Nephrol*. 2014;25(11):2559–2572.
25. Hodgin JB, et al. Identification of cross-species shared transcriptional networks of diabetic nephropathy in human and mouse glomeruli. *Diabetes*. 2013;62(1):299–308.

26. Ju W, et al. Defining cell-type specificity at the transcriptional level in human disease. *Genome Res*. 2013;23(11):1862–1873.
27. Gerbod-Giannone MC, et al. TNFα induces ABCA1 through NF-kappaB in macrophages and in phagocytes ingesting apoptotic cells. *Proc Natl Acad Sci U S A*. 2006;103(9):3112–3117.
28. Zhang Y, et al. Adipocyte modulation of high-density lipoprotein cholesterol. *Circulation*. 2010;121(11):1347–1355.
29. Tejada T, et al. Failure to phosphorylate AKT in podocytes from mice with early diabetic nephropathy promotes cell death. *Kidney Int*. 2008;73(12):1385–1393.
30. Devries-Seimon T, et al. Cholesterol-induced macrophage apoptosis requires ER stress pathways and engagement of the type A scavenger receptor. *J Cell Biol*. 2005;171(1):61–73.
31. Kellner-Weibel G, et al. Effects of intracellular free cholesterol accumulation on macrophage viability: a model for foam cell death. *Arterioscler Thromb Vasc Biol*. 1998;18(3):423–431.
32. Maxfield FR, Tabas I. Role of cholesterol and lipid organization in disease. *Nature*. 2005;438(7068):612–621.
33. Wang Y, et al. Activation of NFAT signaling in podocytes causes glomerulosclerosis. *J Am Soc Nephrol*. 2010;21(10):1657–1666.
34. Harrison BC, et al. The CRM1 nuclear export receptor controls pathological cardiac gene expression. *Mol Cell Biol*. 2004;24(24):10636–10649.
35. Nijenhuis T, et al. Angiotensin II contributes to podocyte injury by increasing TRPC6 expression via an NFAT-mediated positive feedback signaling pathway. *Am J Pathol*. 2011;179(4):1719–1732.
36. Wilkins BJ, et al. Calcineurin/NFAT coupling participates in pathological, but not physiological, cardiac hypertrophy. *Circ Res*. 2004;94(1):110–118.
37. Winslow MM, et al. Calcineurin/NFAT signaling in osteoblasts regulates bone mass. *Dev Cell*. 2006;10(6):771–782.
38. Silverstein DM. Inflammation in chronic kidney disease: role in the progression of renal and cardiovascular disease. *Pediatr Nephrol*. 2009;24(8):1445–1452.
39. Tsukada N, Miyagi K, Matsuda M, Yanagisawa N, Yone K. Tumor necrosis factor and interleukin-1 in the CSF and sera of patients with multiple sclerosis. *J Neurol Sci*. 1991;104(2):230–234.
40. Vernooy JH, et al. Local and systemic inflammation in patients with chronic obstructive pulmonary disease: soluble tumor necrosis factor receptors are increased in sputum. *Am J Respir Crit Care Med*. 2002;166(9):1218–1224.
41. Pierine DT, et al. Lycopene supplementation reduces TNF-α via RAGE in the kidney of obese rats. *Nutr Diabetes*. 2014;4:e142.
42. Trachtman H, et al. Efficacy of galactose and adalimumab in patients with resistant focal segmental glomerulosclerosis: report of the font clinical trial group. *BMC Nephrol*. 2015;16:111.
43. Yoo TH, et al. Sphingomyelinase-like phosphodiesterase 3b expression levels determine podocyte injury phenotypes in glomerular disease. *J Am Soc Nephrol*. 2015;26(1):133–147.
44. Enocsson H, Wetterö J, Skogh T, Sjöwall C. Soluble urokinase plasminogen activator receptor levels reflect organ damage in systemic lupus erythematosus. *Transl Res*. 2013;162(5):287–296.
45. Wei C, et al. Circulating urokinase receptor as a cause of focal segmental glomerulosclerosis. *Nat Med*. 2011;17(8):952–960.
46. Delville M, et al. A circulating antibody panel for pretransplant prediction of FSGS recurrence after kidney transplantation. *Sci Transl Med*. 2014;6(256):256ra136.
47. Savin VJ, et al. Renal and hematological effects of CLCF-1, a B-cell-stimulating cytokine of the IL-6 family. *J Immunol Res*. 2015;2015:714964.
48. Saurus P, et al. Podocyte apoptosis is prevented by blocking the Toll-like receptor pathway. *Cell Death Dis*. 2015;6:e1752.
49. Lassenius MI, et al. Bacterial endotoxin activity in human serum is associated with dyslipidemia, insulin resistance, obesity, and chronic inflammation. *Diabetes Care*. 2011;34(8):1809–1815.
50. Stanley AC, et al. The Rho GTPase Rac1 is required for recycling endosome-mediated secretion of TNF in macrophages. *Immunol Cell Biol*. 2014;92(3):275–286.
51. Yabal M, et al. XIAP restricts TNF- and RIP3-dependent cell death and inflammasome activation. *Cell Rep*. 2014;7(6):1796–1808.
52. Tall AR, Yvan-Charvet L. Cholesterol, inflammation and innate immunity. *Nat Rev Immunol*. 2015;15(2):104–116.
53. Field FJ, Watt K, Mathur SN. TNF-α decreases ABCA1 expression and attenuates HDL cholesterol efflux in the human intestinal cell line Caco-2. *J Lipid Res*. 2010;51(6):1407–1415.
54. Chang YC, Lee TS, Chiang AN. Quercetin enhances ABCA1 expression and cholesterol efflux through a p38-dependent pathway in macrophages. *J Lipid Res*. 2012;53(9):1840–1850.
55. Pramanik R, et al. p38 isoforms have opposite effects on AP-1-dependent transcription through regulation of c-Jun. The determinant roles of the isoforms in the p38 MAPK signal specificity. *J Biol Chem*. 2003;278(7):4831–4839.
56. Fazio S, et al. Increased atherosclerosis in LDL receptor-null mice lacking ACAT1 in macrophages. *J Clin Invest*. 2001;107(2):163–171.
57. Zimmer S, et al. Cyclodextrin promotes atherosclerosis regression via macrophage reprogramming. *Sci Transl Med*. 2016;8(333):333ra50.
58. Isnard Bagnis C, et al. Long-term renal effects of low-dose cyclosporine in uveitis-treated patients: follow-up study. *J Am Soc Nephrol*. 2002;13(12):2962–2968.
59. Fornoni A, et al. Rituximab targets podocytes in recurrent focal segmental glomerulosclerosis. *Sci Transl Med*. 2011;3(85):85ra46.
60. Cherney DZ, Scholey JW, Sochett E, Bradley TJ, Reich HN. The acute effect of clamped hyperglycemia on the urinary excretion of inflammatory cytokines/chemokines in uncomplicated type 1 diabetes: a pilot study. *Diabetes Care*. 2011;34(1):177–180.
61. Sampson MG, et al. Integrative genomics identifies novel associations with APOL1 risk genotypes in black NEPTUNE subjects. *J Am Soc Nephrol*. 2016;27(3):814–823.
62. Saleem MA, et al. A conditionally immortalized human podocyte cell line demonstrating nephrin and podocin expression. *J Am Soc Nephrol*. 2002;13(3):630–638.
63. Fitzgerald ML, Mendez AJ, Moore KJ, Andersson LP, Panjeton HA, Freeman MW. ATP-binding cassette transporter A1 contains an NH2-terminal signal anchor sequence that translocates the protein's first hydrophilic domain to the exoplasmic space. *J Biol Chem*. 2001;276(18):15137–15145.
64. Mendez AJ. Cholesterol efflux mediated by apolipoproteins is an active cellular process distinct from efflux mediated by passive diffusion. *J Lipid Res*. 1997;38(9):1807–1821.
65. Khera AV, et al. Cholesterol efflux capacity, high-density lipoprotein function, and atherosclerosis. *N Engl J Med*. 2011;364(2):127–135.
66. Timmins JM, et al. Targeted inactivation of hepatic Abca1 causes profound hypoalphalipoproteinemia and kidney hypercatabolism of apoA-I. *J Clin Invest*. 2005;115(5):1333–1342.
67. Grabner A, et al. Activation of cardiac fibroblast growth factor receptor 4 causes left ventricular hypertrophy. *Cell Metab*. 2015;22(6):1020–1032.
68. Kato H, et al. Wnt/β-catenin pathway in podocytes integrates cell adhesion, differentiation, and survival. *J Biol Chem*. 2011;286(29):26003–26015.